

Review

Colloid Chemistry of Fullerene Solutions: Aggregation and Coagulation

Nikolay O. Mchedlov-Petrosyan *, Mykyta O. Marfunin  and Nika N. Kriklya

Department of Physical Chemistry, V. N. Karazin Kharkiv National University, 61022 Kharkiv, Ukraine; marfunin.n.a@gmail.com (M.O.M.); nkamneva@gmail.com (N.N.K.)

* Correspondence: mchedlov@karazin.ua or nikolay.mchedlov@gmail.com

Abstract: This review article is devoted to the colloidal properties of fullerene solutions. According to generally accepted understandings, all solvents in relations to fullerenes are divided into “good”, “poor”, and “reactive”. We have consistently considered the state of fullerenes in these systems. In “good”, predominantly non-polar aromatic solvents and CS₂, non-equilibrium dissolution methods lead to the formation of colloidal aggregates, whereas the utilization of equilibrium methods results in the formation of molecular solutions. The latter, however, have some unusual properties; new results considered in this review confirm previously expressed ideas about colloidal properties of these solutions. In “poor” (polar) solvents, lyophobic colloidal systems appear. Both “bottom-up” and “top-down” methods of preparation are well documented in the literature. However, *N*-methylpyrrolidine-2-one, DMSO, and DMF dissolve fullerenes quite easily and with less energy consumption. These solvents can be considered a subset of “poor” solvents that have some features of being “reactive” at the expense of basic properties. New data confirm that hydrosols of fullerenes are typical hydrophobic colloids that obey the Schulze–Hardy rule and other regularities in the presence of electrolytes. Organosols in acetonitrile and methanol are much less stable with respect to the effects of electrolytes. This allows us to assume a non-DLVO stabilizing factor in the hydrosols. Accordingly, a new estimate of the Hamaker constant of fullerene–fullerene interaction is proposed. In DMSO and DMF, the coagulation of fullerene sols is hindered due to strong solvation with these basic solvents.

Keywords: fullerenes; “good” and poor solvents; aggregate formations; organosols; hydrosols; coagulation by electrolytes; overcharging of colloidal particles; Hamaker constant



Citation: Mchedlov-Petrosyan, N.O.; Marfunin, M.O.; Kriklya, N.N. Colloid Chemistry of Fullerene Solutions: Aggregation and Coagulation. *Liquids* **2024**, *4*, 32–72. <https://doi.org/10.3390/liquids4010002>

Academic Editor: Enrico Bodo

Received: 10 October 2023

Revised: 14 December 2023

Accepted: 20 December 2023

Published: 25 December 2023



Copyright: © 2023 by the authors. Licensee MDPI, Basel, Switzerland. This article is an open access article distributed under the terms and conditions of the Creative Commons Attribution (CC BY) license (<https://creativecommons.org/licenses/by/4.0/>).

1. Introduction

At present, fullerenes C₆₀, C₇₀, etc., belong to the most explored chemical compounds, and their study continues. For example, they are used in solar cells [1–3], in creation of nanowhiskers for various areas [4], as additives to the working fluids of refrigerators [5], etc. Their application in various branches of scientific research and technology is often associated with the use of these compounds in solutions. Water-based systems are examined in order to reveal the antioxidant properties of fullerenes [6] and biocompatibility [7,8] to study the environmental impact and related problems [9–11]. Therefore, different modifications and improvements of the introduction of fullerenes into water were proposed [12–16]. The peculiar properties of fullerene solutions in various liquid media are the subject of many publications, including reviews [17–21]. There are also several reviews on this topic by one of the authors of this article [22–25], and therefore we will not repeat much of what is considered in detail in these articles.

The purpose of this review is, on the one hand, to consider the state of the arts. On the other hand, we summarize the results of the work carried out in this laboratory from 1997 to 2022. The focus will be on the colloidal aspect, which is a key to understanding fullerene liquid solutions. We do not consider here either solutions of fullerenes obtained by using surfactants, calixarens, cyclodextrins, etc., or covalently modified fullerenes. We will only discuss the binary systems fullerene–solvent.

2. Solubility of Fullerenes

2.1. “Good”, “Poor”, and “Reactive” Solvents

The first quantitative estimations of C_{60} solubility in different liquids made by Sivaraman, Matthews and coworkers [26,27], and Ruoff [28] have already shown that these values are very low in any solvent. This was confirmed by other authors [29–32]. Soon, a significant amount of data was accumulated on the solubility on fullerenes in solvents of various natures, including temperature dependences of solubility [20,33–36]. The solubility even in solvents called “good”, or “strong” ones, such as 1-chloro-; 1-phenyl-; and 1-methylnaphthalene, 1,2-dichlorobenzene; tetraline; xylenes; toluene; benzene; CS_2 , etc., does not reach 0.1 M (hereafter, 1 M = 1 mole dm^{-3}). These solvents may also be referred to as “high-solubility solvents” [37]. Some authors consider as “good” solvents only those where the molar fraction of fullerenes reaches $x_2 = 0.001$ [38]. Polar solvents, including alcohols, belong to the so-called “poor” or “weak” ones. The solubility in such media drops down to $\sim 10^{-5}$ M or even $\sim 10^{-6}$ M. Aliphatic hydrocarbons should also be classified as “poor” solvents.

At the same time, typical colloid solutions, i.e., suspensions and organosols, can appear in such solvents as acetonitrile, acetone, *N*-methyl-pyrrolidine-2-one, ethanol, etc. [17,39–44]. Sun and Bunker, who first revealed the formation of C_{70} aggregates in the toluene–acetonitrile solvent system, considered the new species as clusters, quite different from colloidal ones [45]. However, their next studies [46,47] as well as subsequent research [39,44], make it possible to classify these systems as colloidal. In water, only hydrosols and suspensions are formed [17,20,22–25].

Many basic solvents form complexes with fullerenes. They are, for example, 1-methylpiperazine, 1-methylpyrrolidone, 1-methylpiperidone, trihexylamine, tetrakis (dimethylamine)ethylene [48]. The interactions can be even stronger and result in the formation of covalent bonds in cases of piperazine, homopiperazine, *N,N'*-dimethylethylenediamine, and piperazine [49,50]. Therefore these and some other nitrogen-containing compounds, which readily form covalently modified fullerene molecules, are called “reactive” solvents [24].

2.2. Peculiarities of Fullerenes Dissolution

For solutions that were considered as true (molecular) ones, i.e., non-colloidal, a number of correlations were proposed in order to explain the fullerene solubility with the help of various solvent descriptors, including the QSPR (quantitative solvent-property relationship) approach; this problem was considered in a previous review [24]. In such procedures, it is necessary to take into account the formation of crystal solvates of fullerenes with some solvents [51]. This effect was revealed in connection with the detection of an extremum on the dependence of solubility on temperature in some solvents [52]. According to Beck, “there are two problems concerning the molecular states of fullerenes in solution. One should determine the degree of self-association and determine the nature and extent of interaction between the fullerene and the solvent molecules.” [53].

The analysis of the solubility in respect to the Hildebrand constant of the solvents performed by many authors revealed that the optimal δ_H value is within the range of 18 to 20 $MPa^{1/2}$ [24]. Ruelle et al. [54] stated that the highest solubility of C_{60} corresponds to solvents with $\delta_H = 20.0$. As early as 1993, Ruoff et al. [28] stated that a typical “good” solvent for C_{60} must have a relative permittivity value about $\epsilon_r = 4$, a large refraction index and molecular volume, the δ_H value of 20 $MPa^{1/2}$, and tendency to act as a moderate strength nucleophile. The latter indicates that the fullerene is a kind of a Lewis acid. This feature is important for understanding the stability of C_{60} and C_{70} colloids in respect of electrolytes in polar solvents; see Section 4.2.

A detailed analysis of 1213 solvents was made using the three-dimensional Hansen solvent parameter [38]. The later allows separately estimate three contributions to the Hildebrand constant of the solvent. Using 15 “good” solvents, Hansen and Smith estimated the corresponding contributions for the C_{60} solute that are as follows: 19.7 $MPa^{1/2}$ for

nonpolar dispersion, $2.9 \text{ MPa}^{1/2}$ for permanent dipole–permanent dipole interactions, and $2.7 \text{ MPa}^{1/2}$ for hydrogen bonding interactions [38]. The δ_H value for C_{60} is a square root of the sum of the corresponding squares: $20.1 \text{ MPa}^{1/2}$. Also, 55 additional earlier not experimentally examined liquids were proposed as “good” solvents for C_{60} , where the solubility reaches molar fraction 0.001 [38]. Cataldo calculated the δ_H values for fullerenes from C_{60} ($19.5 \text{ MPa}^{1/2}$) to C_{90} ($\delta_H = 20.7 \text{ MPa}^{1/2}$) [55].

In some theoretical studies, the relation between solvation of a fullerene molecule and solubility has been disclosed. For example, Wang et al. [56] used the molecular dynamics simulation of C_{60} in different solvents to estimate the half-life time of solvent molecules encompassing the fullerene molecule, $t_{1/2}$, as well as other parameters of the solvation shell. A pronounced drop of solubility along with decrease in $t_{1/2}$ in chlorobenzene, toluene, trichloromethane, ethanol, and water was revealed. Further study on fullerene C_{60} and its derivative [6,6]-phenyl- C_{61} -butyric acid methyl ester, $PC_{61}BM$, demonstrated a single time contact characterizing the dynamic stability of angstrom-size solvation shell allows to know the trend of fullerene solubility [57]. Peerless et al. [58] studied the correlation between solvation shell structure, solvate formation, and solubility. Molecular dynamics simulations for C_{60} and $PC_{61}BM$ in nine aromatic solvents have shown the clear dependence of solubility and solution enthalpy on the degree of order of the solvation shell. Quantum-chemical calculations performed by Zhang et al. [59] for C_{60} in “good” solvents demonstrated that the solubility is generally proportional to the intermolecular force between solute and solvent.

If “poor” solvents are included in various considerations, it should be taken into account that the very low solubility, determined experimentally, may reflect the (possible) presence of colloidal species. Note that most of the available solubility data were obtained without checking the presence of colloids. This issue is of special importance for fullerene solutions. Non-equilibrium methods of preparation can readily result in formation of oversaturated solutions and colloids even in “good” solvents [60–62]. This is likely the main reason of a substantial scatter of the published solubility data. By non-equilibrium methods of preparing solutions, we mean intensive mixing, stirring, sonication, etc. For example, Ruoff et al. determined the solubility of C_{60} in benzonitrile to be $5.7 \times 10^{-4} \text{ M}$ [28]. Five years later, Nath et al. firmly proved the appearance of ca. 250 nm-sized aggregates at fullerene concentration over $1 \times 10^{-4} \text{ M}$ [63].

Interestingly, the solubility value of fullerenes in dimethylsulfoxide (DMSO) is absent in the available data summaries, though C_{60} and C_{70} solutions in DMSO and DMSO–water mixed solvent were already used in 1993 for spreading fullerenes at the water/air surface [64]. Accordingly, DMSO was not included in the correlations between solubility and solvent descriptors. In 2013, Pushkarova and Kholin [65] analyzed the solubility of C_{60} at $25 \text{ }^\circ\text{C}$, basing on Kohonen and probabilistic networks, used a set of nine characteristics of 76 solvents. As a result, they divided the data into eleven solvent groups; DMSO appeared in a group together with *N*-methylpyrrolidine-2-one ($x_2 = 1.2 \times 10^{-4}$), benzonitrile ($x_2 = 6.3 \times 10^{-5}$), nitromethane, and acetonitrile (negligible solubility). As will be demonstrated in Section 4.2, C_{60} readily forms a colloid solution in DMSO.

As for the targeted preparation of colloidal solutions, there are two ways. Formation of colloidal particles occurs either “top-down” or “bottom-up”. The first approach presumes application of sonication, mechanical impact, grinding, trituration, laser beam, etc. The second one consists of the dilution of a stock molecular solution of fullerene in a “good” solvent with a polar solvent. For this purpose, fullerene solutions in toluene, benzene, or CS_2 are often used.

3. Fullerene Solutions in “Good” Solvents as a Platform for Preparation of Colloids

3.1. Precautions for Preparing Molecular Solutions of Fullerenes in “Good” Solvents

It should be noted that even the preparation of fullerene molecular solutions via the equilibrium procedure in “good” solvents is a nontrivial task [21,24,66,67]. For example, Ak-senov et al. revealed a non-monotone change of the total C_{60} concentration in CS_2 solution over time [67]. They explained it by simultaneous passing of dissolution of the solid phase,

aggregation, and sedimentation of large-sized aggregates [67]. Many other examples of such peculiarities of solution preparation can be found in the previous review [24] and references cited therein. After being stored in the dark for at least ten days or, for better results, two weeks, filtering through 220 nm or 450 nm pored filters is necessary, because small pieces of the solid phase can be introduced into the liquid phase. Additional verification of the absence of large-sized species can be made by dynamic light scattering-based methods. Sonication favors clustering of fullerene molecules both in “good” solvents [21,53,60,61] and *n*-hexane [68]. Checking of the presence of oxidation products is also desirable. These products can appear as result of contact with the atmosphere, illumination, and sonication; the oxidation of fullerene molecules can favor the aggregation processes [69]. The most probable admixture in the commercial samples of C₆₀ is C₆₀O. In general, the biography of the initial solid sample can sometimes influence the results. Recently we have mentioned that if the stock solutions of fullerene C₇₀ in benzene or toluene are kept at low temperatures, the colloid systems obtained by dilution with acetonitrile exhibit somewhat different properties [70]. Note that C₆₀ aggregates were observed by other authors when solutions were prepared in benzene and CS₂ at temperature of solvent freezing [71,72].

As an example of UV-visible spectral data, the molar absorptivities of fullerenes in toluene and benzene are presented in Table 1. These values can be used for determination of the concentration of a fullerene in a working solution; they obey the Bouguer–Lambert–Beer law within the concentration range of $(0.06 \text{ to } 6.00) \times 10^{-4} \text{ M}$ [73]. We used the molar absorptivities of C₆₀ for determination of the solubility in benzene and toluene, $(2.04 \pm 0.02) \times 10^{-3}$ and $(3.84 \pm 0.10) \times 10^{-3} \text{ M}$, respectively [73]. Average values of the literature data at 25 °C or room temperature are 2.2×10^{-3} and $3.7 \times 10^{-3} \text{ M}$ [24].

Table 1. The values of λ_{max} , nm and (in parenthesis) molar absorptivity, $E_{\text{max}} \times 10^{-3}, \text{M}^{-1} \text{cm}^{-1}$.

C ₆₀ ^a		C ₇₀ ^b	
Benzene	Toluene	Benzene	Toluene
335 (64.30)	336 (58.43)	333 (45.5)	334 (37.9)
407 (2.962)	407 (3.163)	365 (33.3)	365 (28.7)
541 (0.911)	541 (0.908)	382 (44.5)	383 (37.8)
596.5 (0.809)	596.5 (0.798)	472 (24.5)	473 (21.0) ^c

Note. ^a The values for C₆₀ for 20 °C are taken from ref. [73]. ^b [74] ^c [46,47,75].

The E_{max} value of $21.0 \times 10^3 \text{ M}^{-1} \text{cm}^{-1}$ for C₇₀ in toluene at 473 nm was taken as an average of three publications by Sun, Bunker, and co-authors [46,47,75]. Based on this value, we determined accurate values at 25 °C for other wavelengths [74]. Accordingly, the molar absorptivities of C₇₀ in toluene–benzene mixtures and benzene were estimated. For C₆₀ in benzene and toluene, Gunkin and Loginova [76] reported somewhat lower λ_{max} and E_{max} values as compared with Table 1.

Accurate values for both fullerene solutions in *ortho*-xylene and *ortho*-dichlorobenzene were determined by Törpe and Belton [37]. For example, the λ_{max} , nm ($E_{\text{max}} \times 10^{-3}, \text{M}^{-1} \text{cm}^{-1}$) values for C₆₀ in *ortho*-xylene and *ortho*-dichlorobenzene are 336 (50.63) and 334 (60.37); for C₇₀ they equal 336 (40.61) and 334 (38.83), respectively. In the cited article, an overview of the literature data was presented as well [37]. Data in *n*-hexane were published by Cataldo et al. [77].

Formation of fullerene aggregates in “good” solvents was reported by different research groups. Some authors state that they can be easily destroyed by hand-shaking [78,79], while others report that the aggregation is irreversible [41]. In the last publication, a radical scavenger is used to prevent the aggregation that may occur thorough the disproportionation process. On the other hand, evidence is given for aggregation and nucleation as a result of fullerene interaction with the surface of the flask [41]. According to Bezmelnitsin et al. [80,81], C₆₀ in carbon disulfide behaves as a “cluster substance”. However, it was shown using the SANS (small-angle neutron scattering) method that equilibrium procedure of preparation leads to a C₆₀ molecular solution in CS₂ [21]. Fullerene solutions

in “good” solvents tend to form oversaturated solution, aggregates, and sediment. Based on the SANS method, Avdeev et al. introduced a definition “final quasistationary state of solutions” for low-polarity solvents; small 6 nm-sized clusters can appear near the solubility limit [21]. Using the same method, Török et al. [66] revealed fractal clusters of C₆₀ in toluene at concentrations close to saturation.

3.2. Specific Properties of Molecular Solutions of Fullerenes

Despite the peculiarities mentioned above and some other obstacles, there is a wealth of information on the (unusual) properties of true molecular fullerene solutions in CS₂ and some aromatic solvents. For example, after evaporation of benzene the solid C₆₀ cannot be re-dissolved completely [79]. C₆₀ and C₇₀ in benzene, toluene, and *para*-xylene within the concentration range of 10^{−4} to 0.05 mass % exhibit properties atypical for true solutions [82–84]. The concentration dependence of density is nonmonotonous [82], and the same refers to the relative permittivity [85]. Concentration dependence of boiling point was also reported [86]. Structural ordering by X-ray diffraction studies was revealed by Ginzburg, Tuichiev, and their co-authors long ago and confirmed by ebullioscopy and other methods [82–84]. These investigations were continued [87,88]. They firmly proved that in the boiling process, the number of the solvent molecules related to one solute molecule in the act of phase transition is within the range of ca. 500 to 1000. Different methods allow concluding that for C₆₀ and C₇₀ in benzene, toluene, bromobenzene, 1,2-dichlorobenzene, and *para*-xylene, the single fullerene molecule is surrounded by several hundreds of molecules of aromatic compounds; columns of solvent tens of nanometers long are formed. This is in line with their previous data concerning the large solvation shells deduced from the X-ray diffraction patterns [84]. Zhelezny et al. [89] supported these ideas when studying C₆₀ in *ortho*-xylene. Compressibility studies of C₆₀ solution in toluene allowed deducing that the solvation shell thickness is about 1 nm [90].

A number of important theoretical publications have appeared over the past decade, devoted to the solvation of fullerenes in “good” solvents, including the nature of the solvation shells around the C₆₀ and C₇₀ molecules. These studies confirm in outline the above vision of the fullerene state in “good” solvents [56,91,92]. Fritsch et al. [91] reported the formation of a structured ca. 1 nm-thick toluene layer around a C₆₀ molecule. In another molecular dynamics study, it has been shown that “aromatic solvents are comparatively more structured than the aliphatic ones in close vicinity of C₆₀” [56]. According to quantum-chemical calculations of Li et al., “the $\pi \cdots \pi$ stacking configurations of the complex C₆H₆⋯C₆₀ are more strongly bound than the C–H⋯ π analogues, and the C–H⋯ π interactions in the C–H⋯ π configurations of C₆H₆⋯C₆₀ are not of the hydrogen bond” [92]. These conclusions are based on the quantitative estimations of the interaction energies [92].

These remarkable results can be consisted with previously published theoretical and experimental studies. So, it was shown that the standard entropy values, ΔS^0 , of dissolution and solvation of fullerenes C₆₀ and C₇₀ in “good” solvents are substantially negative [93–97]. For instance, the $\Delta S_{\text{solut}}^0$ values of fullerene C₆₀ dissolution in *ortho*- and *meta*-xylene, bromobenzene, 1,2-dichlorobenzene, CCl₄, and toluene are about $\approx -100 \text{ J mol}^{-1} \text{ K}^{-1}$ [24,94,95]. The solvation entropy for C₆₀ in aromatic solvents, CCl₄, and tetralin is also negative, about $\Delta S_{\text{solvo}}^0 \approx -200 \text{ J mole}^{-1} \text{ K}^{-1}$. Such a sharp decrease in entropy indicates an ordering of the solvent structure, similar to what occurs during the well-known hydrophobic hydration of hydrocarbons in aqueous solutions.

The same can be expected for polar (“poor”) solvents, where the solvophobic nature of fullerene colloids is undisputable [23,24,98–101]. In the recently named systems, it leads to formation of colloidal aggregates owing to solvophobic interactions. Solvophobic properties of solutions of C₆₀ in tetrahydrofurane, benzonitrile, and in other solvents were proved as early as 1992 [102].

The size of the C₆₀, C₇₀, and even more so of higher fullerenes corresponds to the turning point between usual molecules and colloidal particles. They can also be considered as sub-colloidal particles. This allows regarding this kind of nanocarbon as a unique object,

which can be a challenge for application of the common principles of solution chemistry. The most important feature is the structure of fullerenes that makes them impenetrable for solvent molecules. This distinguishes them from many much larger molecules, the separate portions of which are solvated individually.

Therefore, the fullerene molecular solution can also be considered as a kind of a colloid system. The solvation layers around the molecules are thick enough to pronouncedly alter the solvent properties. Such systems resemble the so-called periodic colloidal structures [103–105] or colloidal crystals [106,107]. In other words, according to the DLVO terminology, it looks like a system that is coagulated in the “distant minimum”. Any external influence readily leads to aggregation or deposition.

This issue should be considered in a more detailed way in future. However, as a preliminary conclusion it may be stated that even molecular solutions of fullerenes in “good” solvents exhibit some colloidal features. From the time of Wolfgang Ostwald [108] and Peter von Weimarn [109], it is known that any chemical compound can be, depending on the nature of the solvent, obtained in a colloidal state. Apparently, due to peculiarities of the molecular structure, in particular, due to the extremely high surface atomic density, fullerenes are compounds that exist in a colloidal state or, at least, exhibit colloidal features, in almost any solvent. (Of course, almost infinite dilutions down to “homeopathic” concentrations in any solvent, “good” and “poor”, will result in a true molecular solution, but this is beyond the scope of our discussion).

In addition to the above considered publications, some other interesting articles are worth to consider. Recently, Garcia-Hernandez et al. [110] isolated the complexes of C_{70} with three acenes and characterized them by FTIR, TGA, DSC, and electronic absorption spectra. This again gives evidence of strong interaction between fullerenes and aromatics.

On the other hand, Zhang and Li [111] presented a convincing example of governing the shape of fullerene solid species by evaporation of C_{60} solution in CS_2 under various solvent atmospheres. SEM images demonstrated different architectures of species: belts, sheets, and starfishes depending on the kind of solvent. Twenty different organic liquids were used, which, except for toluene, belong to poor solvents. Previous publications in this direction are also referred to by these authors [111].

3.3. Forced Aggregation of Fullerenes in “Good” Solvents

Until now, we have considered the aggregation of fullerenes rather as a phenomenon that interferes with the preparation of molecular solutions by equilibrium methods. But sometimes prolonged sonication is used consciously to obtain and study aggregates.

Bokare and Patnaik [60,61] purposefully created fullerene aggregates in CS_2 via sonication. Subsequently, Guo et al. [112] prepared C_{60} solutions in toluene and chlorobenzene via sonication 10 h per day at 50 °C for 4 days. SLS/DLS (static and dynamic light scattering), depolarized DLS, SAXS (small-angle X-ray scattering), and cryo-TEM methods were used in order to characterize thus obtained fullerene aggregates. Though all aggregates have the size of several hundred nm, it was revealed that while aggregate clusters are anisotropic in shape in chlorobenzene, they are basically isotropic in toluene. Solvent-induced differences were disclosed by other methods as well [112].

A series of studies with C_{60} and C_{70} fullerenes were performed by Makhmanov et al. [113–116]. Two methods of preparation of C_{60} in toluene, non-equilibrium and equilibrium, were compared [113]. Stirring with a magnetic stirrer within 14 days allowed the authors to obtain porous particles with diameter of 380 ± 20 nm and fractal dimension $D_f = 2.13$. Storing C_{60} in toluene for the same period results in the formation of particles with size ≤ 50 nm, as determined by the TEM and AFM methods. It was revealed that in C_{70} solutions in xylene–tetrahydrofuran, the changes of the refractive index over time reflect the formation and stabilization of colloidal particles [116].

Makhmanov published interesting results for C_{60} fullerene in the xylene–hexane binary solvent [115]. In these solutions, prepared using magnetic stirrer and passed through 220 nm pores, the diameter of colloidal particles reaches 60–70 nm. The measurements

were accompanied by determination of the refractive index; fullerene concentration was 5×10^{-5} M. TEM and DLS methods were used in this investigation. Despite the low ϵ_r values, the author managed to determine the electrokinetic potential of $-(26.6\text{--}28.2)$ mV; solutions were stable up to 72 h.

Bakhramov et al. [4] developed a method of preparation of C_{70} nanowhiskers, $C_{70}NW$, by thermal evaporation of droplets of toluene solutions. The average length of the obtained species was $1.8 \mu\text{m}$ with width up to 175 nm; the shape was confirmed by SEM [4]. Solutions of C_{60} in toluene–tetrahydrofuran were used for fractal coating with thickness up to ca. $1.2 \mu\text{m}$ on a flat dielectric glass surface [114].

Jia et al. [1] improved the formation of high quality homogeneous C_{60} films for preparation of the perovskite solar cells by adding $PC_{61}MB$ in chlorobenzene to C_{60} solutions in *ortho*-xylene to suppress the aggregation of fullerene solutions prepared using sonication.

$PC_{61}BM$ and $PC_{71}BM$ are now very popular because of their use in photovoltaic devices. Therefore, their properties in solutions are intensively studied using both theoretical [2,57,58,117,118] and experimental methods [2]. In the last work, agglomeration of both derivatives was examined in trichloromethane, toluene, chlorobenzene, and 1,8-diiiodooctane using the Spin-Echo Small Angle Neutron Scattering (SESANS) method. The solutions were prepared by intensive stirring at elevated temperature. As a result, formations of large agglomerates were observed for $PC_{61}BM$, but not for $PC_{71}BM$.

3.4. Some Examples of Theoretical Modeling of Fullerene Aggregation

Paliy et al. [118] performed a molecular dynamic study of two C_{60} molecules with a charge of $-5e$ in a trichloromethane droplet, either with or without 10 and 20 Na^+ ions. The results clearly illustrate the regulation of the state of C_{60} molecules with the help of charge. Negatively charged particles, like C_{60}^{5-} , repel each other, particles neutralized by adsorbed counterions stick together and overcharged and thus positive particles repel each other again. Also, the influence of the nanocarbon species on the state of the nanodroplets is studied. The same simulations were made for a carbon nanotube [119]. This is a good explanation of the overcharging phenomenon, which will be considered by us in Section 5.2.

Somewhat earlier than this study, molecular dynamics modelling was also used by Banerjee [120] for fullerenes C_{60} , C_{180} , C_{240} , and C_{540} in toluene, acetone, and water. It was shown that the diffusion coefficient of solvent molecules in the solvation shells is much lower than of those in the bulk liquid. Uncharged fullerene molecules agglomerate in water and acetone, but not in toluene. Introducing a negative charge from $-0.5e$ to $-3e$ per molecule, with Na^+ as counterions, results in repulsion of molecules and significantly reduces agglomeration in polar solvents; in toluene, the sodium ions associate with anions in accordance with the known regularities for electrolytes in non-polar solutions [120]. These theoretical results give a fairly accurate picture of the colloidal properties of fullerenes in solutions.

Mortuza and Banerjee [121] performed a molecular dynamics study of the behavior of $PC_{61}BM$ in toluene, indane, and in mixtures of these two solvents at temperatures between 280 and 320 K with different concentrations of this fullerene derivative. It was demonstrated that large clusters are formed in toluene. Another important work of the same research group was based on the combination of molecular dynamics with kinetic Monte Carlo method [122]. The agglomeration of fullerene species was proved for aqueous $NaCl$ solutions; this article will be considered later in Section 5.1 devoted to coagulation of hydrosols.

4. Formation and Properties of Colloidal Particles in “Good” + “Poor” and “Poor” Solvents

4.1. “Bottom-Up” Procedure of Fullerene Organosols Preparation

The variations of concentration and using different preparation methods, the fullerene spectra in high-solubility solvents stay almost unaffected. Contrary to it, a fundamental

change is observed on going to polar solvents, and the DLS method firmly indicates appearance of colloidal species (Figure 1).

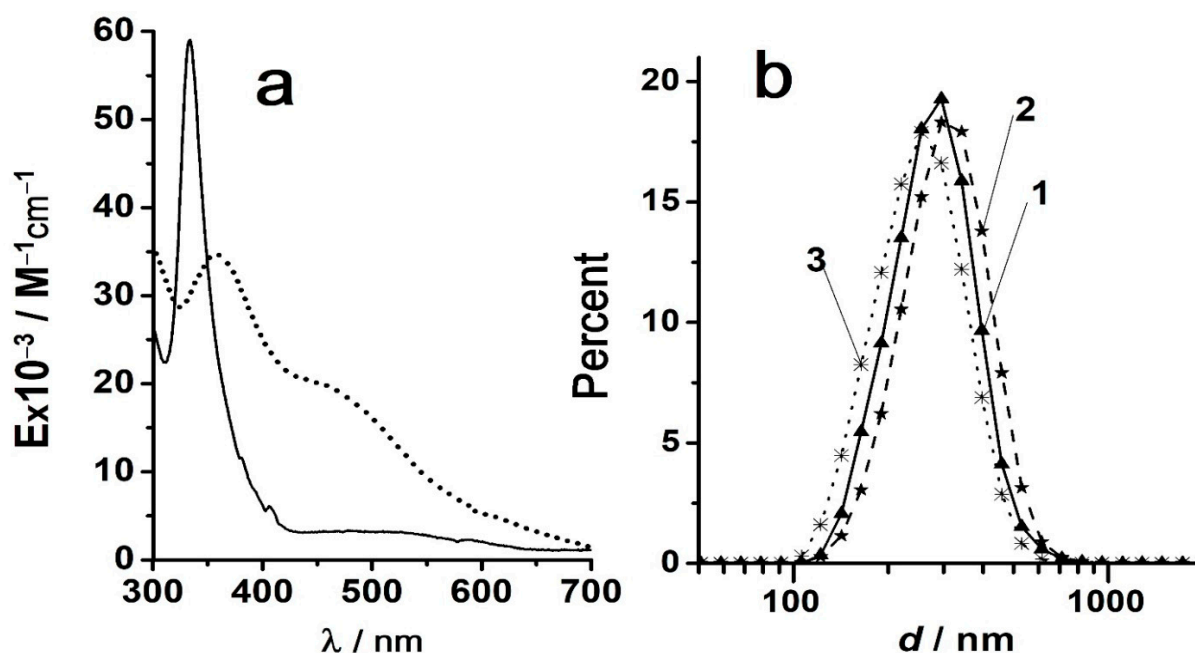


Figure 1. (a) The UV-visible absorption spectra of C₆₀ solutions in toluene (solid line) and in methanol with 1 vol.% toluene (dotted); (b) The particle size distribution in the C₆₀ sol in methanol with 1 vol.% toluene; distribution by intensity (1), volume (2), and number (3). Fullerene concentration: 4×10^{-6} M. Reprinted from ref. [123] with permission.

Let us consider the “bottom-up” procedure. Dilution of molecular solutions with acetonitrile, ethanol, methanol, and other “poor” solvents leads to formation of colloid solutions. In this case, the formation of colloidal species in solutions can be observed using UV-visible spectra. First it was demonstrated in the pioneering work by Sun and Bunker for fullerene C₇₀ in the toluene–acetonitrile binary solvent system [45]. Since then, a number of such studies with C₆₀ and C₇₀ fullerenes was published; benzene, toluene, carbon disulfide, and some other “good” solvents were used for preparation of the initial fullerene solutions [21,39–44,71,72,124–126].

Dilution of a fullerene solution in a polar solvent with another polar solvent is a special case [127] that will be considered below. Some studies were performed in this laboratory [70,73,98,99,101,123]. Figure 2 demonstrates the changes in the UV-visible absorption spectra of C₇₀ in toluene–acetonitrile along with the decrease in the CH₃CN concentration [70,99]. At high acetonitrile content, a contribution of light scattering cannot be ruled out [99].

It is well documented that in the toluene–acetonitrile system, the solvent mixing regime is of key importance [44,46]. For example, dropwise or prompt adding of CH₃CN to a toluene solution of C₇₀ results in principally different absorption spectra of fullerene [46]. Molecule–aggregate transitions of fullerenes are accompanied by changes in fluorescence [39,43,46].

It seems natural to reveal the critical composition of the binary solvent where the colloidal particles appear [45]. Nath et al. [42,43] subjected this problem to detailed study. Basing on a number of binary solvent systems and using the ϵ_r value as a characteristic of the solvent, they stated that C₆₀ forms molecular associates already at ϵ_r about 12–13, while C₇₀ only at ϵ_r 27–31. Such differences are explained by a stronger interaction of C₇₀ with “good” solvents [43]. These critical parameters were determined by both electronic absorption spectra and DLS, and the results agree [42,43]. It should be noted that in these works, the ϵ_r values of mixed solvents were calculated using the additive scheme, which

can lead to some (slight) errors [73]. Also, it is well known that many properties of solutes can substantially differ in isodielectric solvents [128].

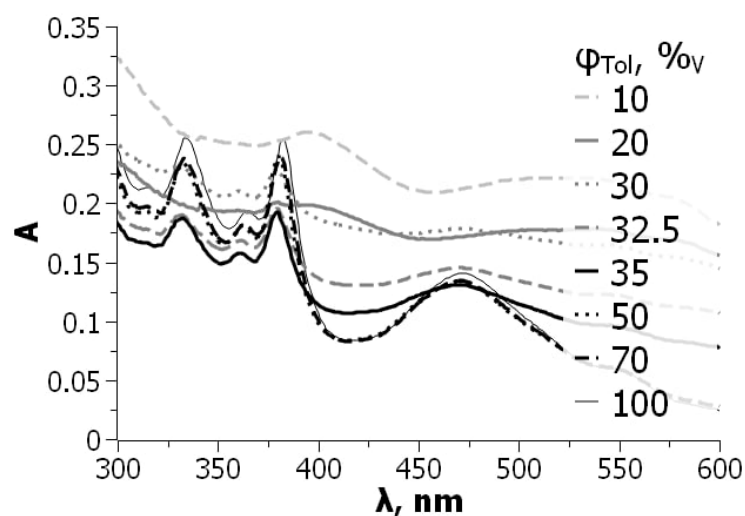


Figure 2. Selected absorption spectra of C_{70} (5×10^{-6} M) in the toluene–acetonitrile solvent system at 25 °C. From ref. [99] with permission.

Two remarks should be made on this. First, even when the DLS method demonstrates the formation of colloidal particles and absence of molecular species, the UV-visible spectra retain the features of molecular absorption [70,73,99,101]. In other words, the onset concentration of the polar co-solvent is somewhat lower as determined by light scattering. For example, for the system presented in Figure 3, the critical content of acetonitrile is 62 vol.% and 64–70 vol.% as obtained by DLS and UV-visible spectroscopy, respectively [99]. Such findings can be explained either by hindering of observation of fullerene molecules in the presence of much stronger light scattering colloidal aggregates or by retaining aromatic solvation shells of fullerenes involved into the aggregates. Note that in a toluene–*n*-hexane solvent system, the absorption spectrum of C_{70} changes gradually along with rise of the aliphatic component, whereas no sign of colloidal particles is observed. This phenomenon is obviously caused by replacing the toluene molecules in the primary solvation shells of C_{70} by *n*-hexane [99] and of C_{60} by dichloromethane [129].

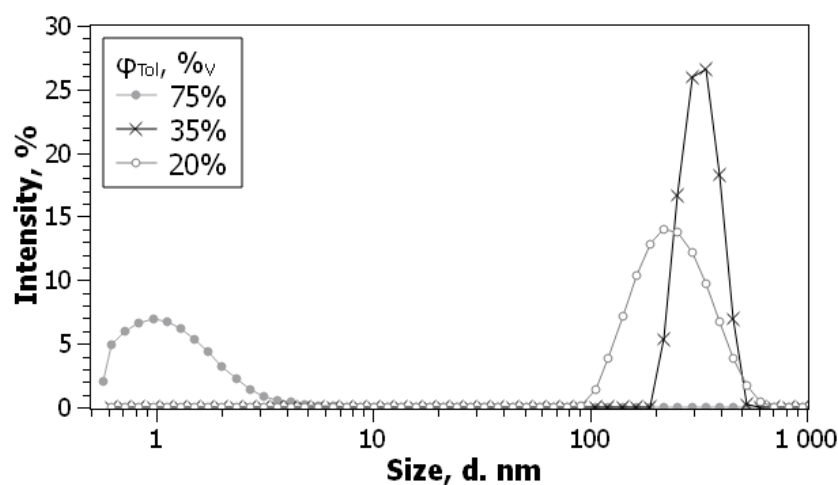


Figure 3. Examples of particle size distribution (by intensity) C_{70} (5×10^{-6} M) in the toluene–acetonitrile solvent system at 25 °C. From ref. [99] with permission.

Second, the fullerene concentration is an important factor. Sun and Bunker [45] mentioned that in a toluene–70% acetonitrile mixture, the absorption spectrum of C_{70} at concentration $\leq 8 \times 10^{-8}$ M is close to that in neat toluene. We confirmed this early statement using the DLS method: at C_{70} concentration of 1.2×10^{-7} M under the same conditions, only species with a size of ca. 1 nm were found [70,99].

A more detailed consideration of the formation of fullerene colloidal species in the toluene–methanol system [73] reveals that the size of the aggregates decreases along with the increase in the polar solvent fraction. This is in accordance with the classical regularity formulated by Volmer [130]: the lower the solubility is, the smaller the colloidal particles are formed. However, if the initial toluene solution of C_{60} is prepared by a non-equilibrium method and oversaturated, the situation observed for a toluene–acetonitrile solvent system can be reverse [129].

Interestingly, Pille et al. [131] considered the alterations of the C_{60} UV-visible absorption spectra on adding acetic acid, acetonitrile, methanol, DMSO, and DMF to a 1.3×10^{-3} M toluene solution in terms of preferential solvation, not aggregation. The stock solution was prepared using stirring and sonication.

Recently, Kyzyma et al. [129] conducted a detailed study of the C_{60} –toluene–acetonitrile system using the UV-visible absorption spectra, TEM, DLS, SLS, SAXS, SANS, and LDI mass-spectrometry. Two series of experiments were performed, starting with C_{60} solutions in toluene prepared by equilibrium and non-equilibrium (sonication) methods. The C_{60} working concentrations were $(4.0\text{--}6.3) \times 10^{-6}$ and $(0.23\text{--}1.9) \times 10^{-3}$ M, respectively. In all cases, adding of acetonitrile to the toluene solutions of C_{60} favors aggregation. It is firmly proved that oxidation and illumination display pronounced influence on the aggregation processes. In the cited article [129], the obtained data are compared with the results published by others.

In entire benzonitrile and benzyl alcohol, a threshold concentration of fullerene C_{60} aggregation was reported [63]. These polar solvents belong to the aromatic ones. For example, in benzonitrile, a solvent with $\epsilon_r = 26$, colloidal ≈ 250 nm-sized particles appear at 1×10^{-4} M. Note that ultrasonication was used for preparation; larger particles may be removed by centrifugation and decantation [63]. This critical concentration was estimated by both DLS and visible spectra at $\lambda = 450\text{--}700$ nm; the $nC_{60} \rightleftharpoons (C_{60})_n$ equilibrium is reversible [63]. This is typical rather to lyophilic systems, like diphilic surfactants in water, which are characterized by a critical micelle concentration, CMC. However, the fundamental difference consists of the limiting solubility (here, it is 5.7×10^{-4} M [28,35]), whereas for common surfactants in water, after reaching the CMC, the micellar solubility rises up to gelation. On the other hand, as it was mentioned in Section 3.1, small fullerene aggregates can appear near the solubility limit even in “good” solvents [21]. Obviously, the same takes place for the C_{60} solutions in benzonitrile.

For C_{60} in the toluene–acetone binary solvent system, the effects are similar to those observed for toluene or benzene mixtures with acetonitrile [73]. If a benzene solution of C_{70} is diluted by DMSO, the spectral changes resemble those presented in Figure 2. At DMSO content of 33 vol.%, no sign of colloidal particles is observed (Figure 4). The turning point of molecule–aggregate transition is about 60 vol.% DMSO [74].

It should be noted that, contrary to the mixtures of a “good” solvents with methanol and acetonitrile, the size colloidal particles does not decrease near 100% DMSO. Obviously, DMSO plays another role compared to “poor” solvents, due to good solvation of C_{70} molecules. The properties of the DMSO-based systems will be considered in the next sections.

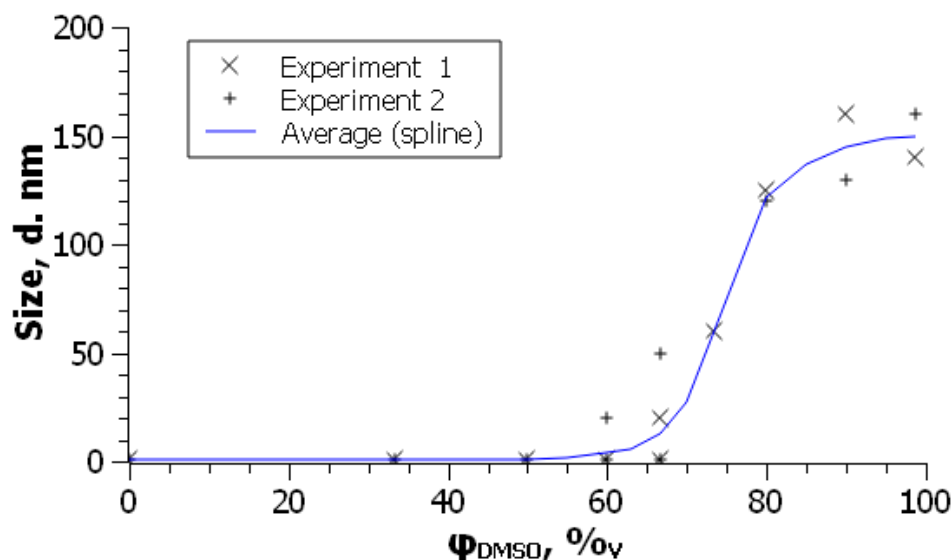


Figure 4. Dependence of particles size of C_{70} (5×10^{-6} M) on the composition of the benzene—DMSO binary solvent. Results of two independent experimental series were obtained immediately after preparation of solutions. From ref. [74] with permission.

4.2. “Top-Down” Preparation of Organosols and Suspensions

Another way is the “top-down” preparation. This means the breaking, grinding, mixing, and stirring of a solid sample in a polar solvent. Sonication and laser beam treatment can be also used. A more practical procedure was developed by Deguchi and Mukai [132]. The “top-down” preparation of C_{60} colloids in methanol, ethanol, 1-propanol, 2-propanol, 1-octanol, acetonitrile, and acetone was performed using 1–2 min hand-grinding of the solid sample in an agate mortar and sonication in a “poor” solvent [132]. Furthermore, the same research group used this procedure to obtain stable graphite dispersion in aqueous acetone [133].

We have repeated this protocol for C_{60} in acetonitrile with some modifications [100,129]. The size of particles as determined by DLS is 200–300 nm, in agreement with Deguchi and Murai [131] and with our TEM data. The size distribution by number, scattering volume, and intensity is similar; the repeatability is medium, the polydispersity index, PDI, is 0.3 on average. Dilution with benzene (Figure 5) allowed determination of the initial fullerene concentration in acetonitrile of ca. 3×10^{-5} M.

Fullerene C_{60} and C_{70} solutions in *N*-methylpyrrolidine-2-one, NMP ($\epsilon_r = 32$), are a special case [17,21,125–127,134–148]. While dilution of fullerene solutions in toluene, benzene, or CS_2 by acetonitrile, acetone, or alcohols is quite understandable from the point of view of colloid chemistry as an example of “bottom-up” preparation, the “top-down” preparation of fullerene colloids in the last “poor” solvents needs sonication. However, sonication is unnecessary in NMP. In earlier studies [125,126], C_{60} and C_{70} solutions in toluene were diluted with NMP in order to prepare colloidal solutions. Also, sonication was used for the preparation of fullerene solutions in toluene, toluene–NMP mixtures, and in entire NMP. In other cited papers, the fullerene solutions were prepared directly by stirring the solid sample in NMP. The stirring time varied from 10–15 min [138,140,143,146,147] to 1 h [136,139,144], 6 h [141], 24 h [127] or four days [135]. In some studies, initial solutions for investigation of the NMP–toluene systems were prepared either in toluene or in both polar and “good” nonpolar solvents [140,143–145].

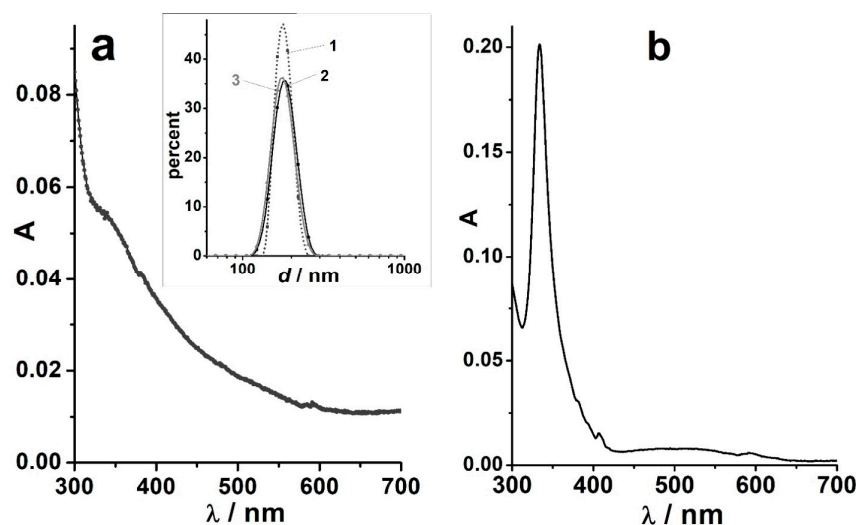


Figure 5. The absorption spectra of C_{60} colloid in acetonitrile, obtained by a 5 min hand grinding and 90 min sonication in an apparatus with electrical power ca. 50 W and frequency 40 kHz and additionally dilute (a) and the solution diluted 10-fold by benzene (b); insert in the left-hand side: particle size distribution by intensity (1), by volume (2), and by number (3). From ref. [100] with permission.

Detailed studies of C_{60} [134–136,138–141,144,147] and C_{70} [143,145,146] in NMP-based systems made it possible to shed light upon the unusual properties of this solvent in respect to fullerenes. The main specific feature is the strong interaction between the fullerene and solvent molecules. Obviously, it is a kind of donor–acceptor interaction, which results in formation of charge transfer complexes [139,141,144,147] proved by the 1H NMR spectroscopy, quantum-chemical calculations [139,144], and mass spectra [135,144]. Another property is ageing of fullerene solutions over time, slow increasing in size up to ca. 500 nm as determined by DLS, SANS, and SAXS methods. The UV-visible spectra exhibit some bands characteristic for molecular absorption, but after preparation of solutions, smoothing of the absorption curve begins immediately, and the spectrum strongly resembles that shown in left hand side of Figure 5. Importantly, using some assumptions it was demonstrated that the Mie light scattering makes a negligible contribution in this case [135].

Sun et al. [149] studied the behavior of C_{60} and C_{70} in entire triethylamine. The UV-visible spectra of the solutions prepared either by sonication or without it exhibit a smooth curve. UV-visible spectra of freshly prepared solutions exhibit some features of molecular absorption. However, within 2 h, the spectra curve became completely structureless, like in the above mentioned case of NMP. However, the authors assume that the origin of the absorption changes is a chemical reaction, not a complex formation. This point of view is based on the NMR spectra and fluorescence data. This allows classifying triethylamine as a “reactive” solvent.

Returning to the NMP, it should be concluded that, in any case, the reason for the ease of dissolution is the strong interaction of this electron-donor solvent with fullerenes. In toluene–NMP binary solvents, formation of 55–60 nm particles occurs within ca. 1 h [125,126]. A set of works were devoted to absorption spectra of fullerenes in the toluene–NMP system at different sequence of components adding [125,126,140,141,143–146]. These data demonstrate peculiarities of competition between these two solvents in the solvation shells of fullerene molecules. Because of some information on the irreversible changes of the fullerene solutions [140], the NMP may be (partly) attributed to the “reactive” ones.

Some studies were devoted to kinetics of fullerene aggregation [21,150]. The nucleation process was studied in detail by Tropin, Avdeev, Aksenov, and their colleagues in NMP [21,137,142,151,152]. These authors managed to describe the experimental data using the model of complex formation between fullerene and solvent.

Obviously, the electron-donor properties of solvents are of the crucial role in solvation of fullerenes, which are Lewis acids [74]. While the value of the relative permittivity, ϵ_r , is used to characterize the solvent polarity, the Gutmann's donor number, DN, describes the cationophilic properties [128,153]. In Table 2, both parameters for some selected solvents are given (mainly at 25 °C).

Table 2. Solvent characterization from ref. [128].

Solvent	ϵ_r	DN
Benzonitrile	25.2	11.9
Acetonitrile	35.9	14.1
Acetone	20.6	17.0
Methanol	32.7	19.1 ^a
Water	78.4	24.3 ^a
DMF	36.7	26.6
NMP	32.2	27.3
DMSO	46.4	29.8
Triethylamine	2.42	31.7
Pyridine	12.9	33.1

Note. ^a Approximate estimates.

Among the non-hydrogen bond donor solvents, the first three in Table 2 are typical protophobic (cationophobic) ones, while the last five are protophilic (cationophilic). Pyridine dissolves the C₆₀ fullerene, and aggregates were observed via DLS [154]. The preparation of solutions of C₆₀ in DMF was described by at least two research groups [155,156]. However, recently the colloidal solutions in this solvent were obtained even easier [74]. Note that some organic solvents may become unstable over time. For example, DMF can decompose to formic acid and dimethylamine [157]. In our study, we used freshly purified and distilled DMF.

Although solutions of fullerenes in DMSO and DMSO–water solvents were already obtained in 1993 and were used for spreading at the water/air interface [64], these systems were not further considered in more detail. Wang et al. [64] reported no details of the preparation of solutions. For DMSO, the sonication is undesirable (After even several minutes of sonication, substantial amounts of acidic admixtures appear in DMSO; colloidal particles of fullerenes became positively charged and unstable [74].) but fortunately not necessary [74], analogous to the case of NMP. We prepared C₆₀ and C₇₀ colloidal solutions in DMSO and DMF by hand grinding in an agate mortar and 3 h mixing with a magnetic stirrer [74]. The solutions are rather stable over time and contain \approx 200–250 nm-sized particles with substantially negative electrokinetic potential. The repeatability of the preparation procedure was good.

UV-visible absorption spectra are typified in Figure 6. Particle sizes and size distribution do not undergo major changes over time. In the freshly prepared solutions of C₇₀ in DMF, the molecular bands are observed with the λ_{\max} , nm ($E_{\max} \times 10^{-3} \text{ M}^{-1} \text{ cm}^{-1}$) values of 331 (55.7); 360 (43.2), 380 (56.0), and 467 (31.4). However, smoothing of the spectral curve begins shortly after the preparation of solutions. For the C₆₀ solution in DMF, typical molecular band of 332–333 nm was observed immediately after preparation.

Similar results were obtained in DMSO: C₇₀ exhibits molecular bands of 333, 363, 380, and 470 nm, and smoothing of the curve takes place (Figure 7).

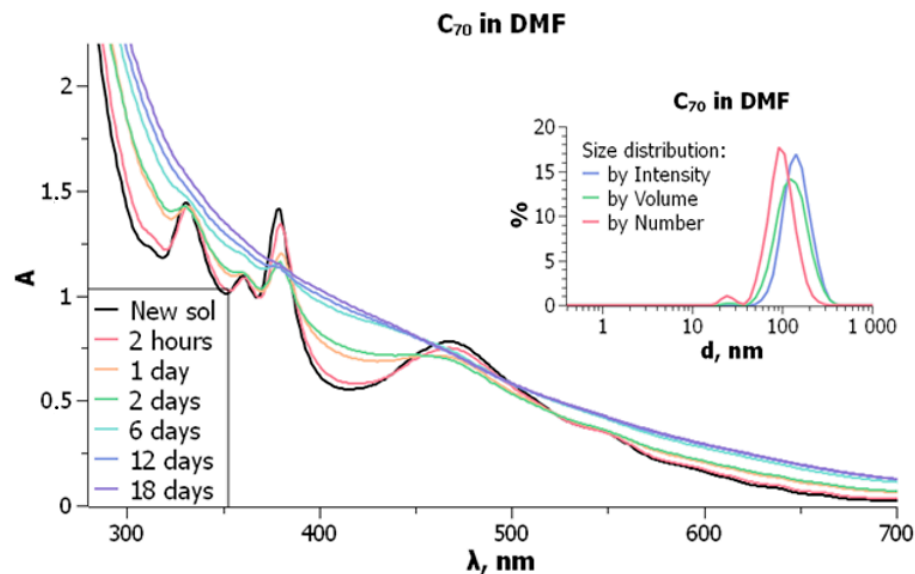


Figure 6. Absorption spectra of fullerene C_{70} , 2.5×10^{-5} M, in DMF over time. Insert: particle size distribution of the same solution, freshly prepared. From ref. [74] with permission.

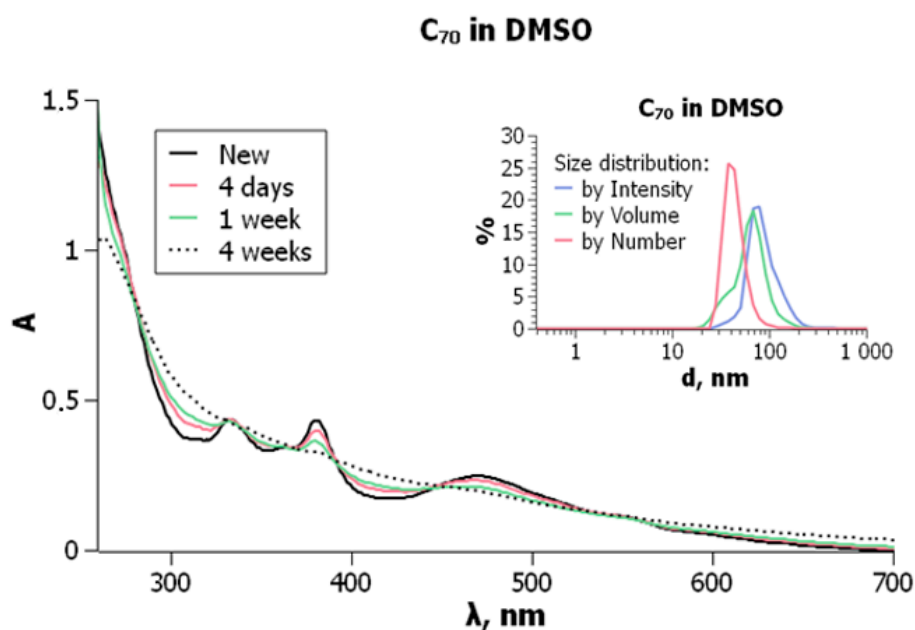


Figure 7. Absorption spectra of fullerene C_{70} , 9.6×10^{-6} M, in DMSO. Insert: particle size distribution of the same solution, freshly prepared. From ref. [74] with permission.

Despite a significant variety of solvent compositions of organosols (suspensions) of fullerenes, they have one important property in common. Namely, colloidal particles are always negatively charged [44]. Now we have a set of electrokinetic potential values in different solvents, calculated using the Henry equation (Ohshima approximation) [158,159]. They are compiled in Table 3. (The overcharging phenomenon in the presence of electrolytes will be considered in Section 5).

Table 3. Values of the electrokinetic potential of organosols, 25 °C.

Fullerene	Solvent	ζ , mV ^a	Reference
C ₆₀	Methanol	−37	[123]
—	CH ₃ CN—0.1 vol.% toluene	−53	[98,129,160]
—	CH ₃ CN—0.1 vol.% toluene	−(47–51)	[98,129,160]
—	CH ₃ CN—benzene (1:1 by vol.)	−53	[98,101]
—	DMSO	−34	[74]
C ₇₀	CH ₃ CN—10 vol.% toluene	−55	[70]
—	DMSO	−42	[74]
—	DMSO—10 vol.% benzene	−45	[74]

Note. ^a The accuracy is normally $\pm(3-8)$ mV.

These results are in agreement with the earlier published work by Alargova et al. [44], where the $\zeta = -(32.5-38.5)$ mV in acetonitrile for colloids of C₆₀, C₇₀, and their mixtures was reported. Their calculations were processed using the Smolukhowski equation; for recalculation to the Henry equation, they are $-(48.8-57.8)$ mV.

The origin of the charge of fullerene colloidal species in polar organic solvents is of special interest. The transfer of electrons from the solvent molecules to fullerenes is obviously the most probable path [44]. Also, disproportionation of the C₆₀ molecules into oppositely charged radicals can also take place [41]. In the latter case, it favors aggregation even in a “good” solvent; this process can be suppressed by introducing a radical scavenger [41]. Indeed, we have demonstrated that if a benzene solution of C₆₀ is mixed with an equal volume of acetonitrile in the presence of 2,6-di-*tert*-butyl-4-methylphenol, a substantial decrease in the ζ value, accompanied by a jump of the particle size, takes place [101]. Within a period of 1 h, the average size reaches 1700 nm, and then the precipitation of fullerene takes place, while ζ approaches zero [101]. If, however, the radical scavenger is added at 1.5 h after formation of the colloid, no changes are observed. In a set of C₆₀ colloidal solutions in acetonitrile, prepared by hand-grinding and sonication [100], the ζ value was within the range of $-(42-63)$ mV, average value $\zeta = -48$ mV. If acetonitrile contains a radical scavenger 2,6-di-*tert*-butyl-4-methylphenol, the interfacial charge greatly reduces; ζ is about -10 mV. This further confirms that free radicals are a source of charge formation. Similar but not expressed changes are observed in acetonitrile with 1 vol.% toluene [101]. For C₇₀ colloids, the above effects were almost imperceptible.

Fullerene solutions in polar basic solvents can readily be mixed with water. This was demonstrated by Mrzel et al. [154] for pyridine. These authors underline the difference between the C₆₀ aggregates in pyridine and nanocapsulates of fullerene in pyridine–water mixtures [154]. DMSO-based organo-hydrosols of C₆₀ and C₇₀ were prepared by Wang et al. [64] and in our study [74]. Chaban et al. [161] studied the C₆₀–water–DMSO system using the molecular dynamics simulations and predicted good solvation of fullerene molecules by DMSO and fullerene aggregation. The same was demonstrated for the DMF–water systems [74]; Yang et al. [156] added water to the C₆₀ deposit after evaporation of DMF, and a hydrosol was obtained. Dilution of fullerene solution in NMP with water also results in organo-hydrosols [135,136,138,146,148]. In all these hybrid sols, the fullerene particles are also negatively charged.

To conclude this section, fullerenes in polar solvents exist as colloidal systems. However, all these solvents exhibit individual features. While methanol, acetonitrile, and acetone are typical “poor” solvents with C₆₀ solubilities of 3.3×10^{-8} , 5.6×10^{-7} , and 1.4×10^{-6} M, respectively [35], for cationophilic DMF, pyridine, and NMP this key parameter is higher: 3.75×10^{-5} , 8.3×10^{-4} , and 1.2×10^{-3} M, respectively [35]. On the other hand, the solubility of C₆₀ in benzonitrile, a polar solvent with the lowest DN value among collected in Table 2, is with 5.7×10^{-4} M substantial. Obviously, the reason is the aromatic nature of this solvent, which favors solvation of fullerenes. Moreover, just in this solvent single fullerene molecules predominate within a pronounced concentration range, before the aggregation is observed [63]. The same was reported by Nath et al. for the benzyl alcohol [42]; these authors underline the “intermediate” character of polar aromatic solvents. It can be argued

that even for the few organic liquids discussed above, it is possible to divide them into three sub-groups of “poor” solvents.

Though NMP should be considered rather as a “poor” solvent, with some features of “reactive” ones, Stuart et al. [127] prepared a C₆₀ solution in acetonitrile by ten-fold dilution of the initial NMP solution with another “poor” solvent CH₃CN. Alargova et al. [44] consider NMP as a polar solvent, which “exhibits good solubility of C₆₀ (comparable to that in toluene), being an exception among the “good” solvents for fullerenes.” Their experiments showed that dilution of C₆₀ solution in NMP with acetonitrile resulted in the formation of colloidal particles similar to those obtained using aromatic solvents instead of NMP [44]. However, it was firmly proved that, despite relatively easy dissolution of fullerenes in NMP, all solutes within a short interval of time transfer into colloidal state [134–136,138–141,143–147]. The same is true, e.g., for DMSO [74].

So, if such solvents can be classified as “high-solubility” to some extent, they dissolve fullerenes only in the form of colloidal aggregates. On the contrary, aromatic solvents dissolve fullerenes in molecular form under equilibrium conditions.

4.3. Fullerenes in Room Temperature Ionic Liquids, RTIL

Room temperature ionic liquids, RTIL, like fullerenes, have long ceased to be exotic compounds, but their combination has been relatively little studied to date. Theoretical studies on C₆₀ with were performed by Fileti, Chaban, and Maciel [162–165] and Garcia et al. [166,167], whereas Pádua group performed both experimental [168–170] and theoretic studies [168].

In the first article [168], interaction of C₆₀ with four ionic liquids having the same anion, bis(trifluoromethanesulfonyl)amide (Ntf₂[−]), and differing in the lengths of the alkyl chains of the 1-alkyl-3-methylimidazolium cations, from ethyl to *n*-decyl, was described. Solid fullerene was dissolved in CH₂Cl₂ using 5 min sonication and prolonged stirring. After mixing with the RTIL 1-decyl-3-methylimidazolium bis(trifluoromethanesulfonyl)amide and evaporating the molecular solvent, UV-visible spectra at C₆₀ concentrations up to 6.25 × 10^{−4} M demonstrated pronounced difference from that in CH₂Cl₂. Some difference in the behavior of the fluorinated fullerene, C₆₀F₄₈, was observed [168]. In the next study, it was shown that the enthalpy of mixing of decylmethylimidazolium bis(trifluoromethanesulfonyl)amide with 1,2-dichlorobenzene is more negative in case the organic solvent contains C₆₀ [169]. More detailed comparison of C₆₀ and C₆₀F₄₈ demonstrated that their solubilities in [bmim]⁺[Ntf₂[−]] are 7 × 10^{−5} and 6 × 10^{−4} M (here, bmim⁺ means 1-butyl-3-methylimidazolium cation). Whereas colloidal particles of C₆₀ are large, up to 5 × 10⁴ nm and sedimentates even at low concentrations, C₆₀F₄₈ exists as solvated isolated molecules or small aggregates and sedimentates only at concentration of 1.5 g/L. However, the smoothing of absorption curve also takes place for C₆₀F₄₈.

The solubility of C₇₀ in imidazolium-, ammonium-, and phosphonium-based RTIL was found even earlier in the course of fluorescence studies; Cl[−] and Ntf₂[−] were used as counter ions [171]. The procedure was as described above. The solubility of C₇₀ varied from 0 in [bmim⁺][BF₄[−]] to 9.5 × 10^{−5} M in [methyltrioctylammonium⁺][Ntf₂[−]]. Although the authors exclude the formation of suspensions, this conclusion is probably based on visual observation. In any case, the absorption curve is smooth. Hence, some kinds of aggregates seem to be probable.

Maciel and Fileti [162] used molecular dynamics simulations for estimating the solvation energy of C₆₀ in ethylammonium nitrate and 1-butyl-3-methylimidazolium tetrafluoroborate. The solvation of the fullerene by nitrate is substantially better than by the BF₄[−] ion. The energy of C₆₀ transfer from the first to the second RTIL was estimated as 235 kJ mole^{−1} (±1%) [162]. The modeling predicts separation of two C₆₀ by a bmim⁺ cation [163,164]. At the same time, fullerenes are Lewis acids. In the last work, Fileti and Chaban theoretically predicted a jump of the C₆₀ solubility in [bmim⁺][BF₄[−]] at high temperatures, up to 380 K [164]. This interesting conclusion should be verified experimentally.

Garcia et al. [166,167] presented important results on analyzing the interactions of 24 different RTIL with C_{60} using molecular dynamics and DFT methods. Structural, dynamic, and energetic factors were analyzed to clarify their role on the behavior of the above systems. In particular, the role of the π - π interactions is important, which is in line with other theoretical considerations [162–164]. Useful guidelines are provided for selecting an RTIL suitable for fullerene solvation; rationalization means an adequate cation-anion choice [167].

Recently, Cardoso and Colherinhas [172] published a detailed molecular dynamics investigation of C_{60} with [bmim⁺][PF₆⁻] and water, using polarization effects. In order to observe the impact of fullerene–solvent electronic interactions, the NMR and electronic absorption spectra were calculated using the GIAO-DFT and TD-DFT methodology [171]. These authors also compared the solvation of C_{60} in water, DMSO, and DMF and demonstrated a better solvation in the last organic solvents [171].

It can be concluded that in RTIL, also known as “green” solvents due to their negligible vapor pressure, the C_{60} and C_{70} fullerenes exist in form of aggregates. As for the permittivity of RTIL, even estimating this value is not an easy task. For [bmim⁺][PF₆⁻] and estimate $\epsilon_r \approx 10$ can be accepted [173,174]. Hence, the RTIL solvents are on the border between polar and non-polar ones; they should be ascribed to “poor” solvents. Also, the large variability of RTIL should be taken into account; in this case, the above mentioned theoretical modeling can be useful for correct choice of solvents.

Campisciano et al. [175] covalently attached imidazolium groups to the C_{60} molecule and thus obtained a valuable supramolecular system for providing Suzuki and Mizoroki–Heck reactions in aqueous media. The smoothing of the spectral curve in the UV-visible range is pronounced. In any case, such a modification makes it possible to transfer the fullerene to water. Basing on molecular dynamics method, Fileti and Chaban [165] recommended the imidazolium ionic liquid [bmim⁺][BF₄⁻] for dispersion of fullerene in water. In this sense, the RTIL is one of the ionic compounds capable of stabilizing colloidal fullerene particles in hydrosols.

4.4. Hydrosols of Fullerenes: Preparation

In water, fullerenes exist in colloid state. Because the electrophilic properties of C_{60} and C_{70} are pronounced, a number of studies were directed to their biological activity and possible application in medicine [6,9,11,12,14,15,176,177]. On the other hand, a plenty of information on cytotoxicity, photocytotoxicity, genotoxicity (DNA damage), etc., is available [24,25]. Many studies are devoted to the behavior of fullerenes in soils, freshwater, etc. [9,10,16,177–180].

As a result, an impressive number of different procedures and protocols of preparation of fullerene hydrosols and aqueous suspensions is accumulated; see, e.g., recent review papers [15,16,24,25]. This set of methods that have been tried for the preparation of hydrosols and aqueous suspensions of fullerenes can serve as an excellent teaching example for a university course in colloid chemistry.

Some of the colloidal solutions are rather suspensions than sols, first of all those prepared by “top-down” method, whereas hydrosols are first of all prepared by the “bottom-up” way. However, following many authors, we use these terms here mainly as synonyms. For orientation in this dataset, special designations for the most popular preparation methods gradually appeared, such as, e.g., son/ nC_{60} . Here “son” and “ nC_{60} ” denote sonication and aggregate formation, respectively.

First approach was the stepwise solvent exchange going from C_{60} in benzene to tetrahydrofuran, then to acetone, and finally to water; the final fullerene concentration was 2×10^{-6} M [181]. If the initial fullerene solution is prepared in toluene and successively diluted with tetrahydrofuran, acetone, and water, the target system is designated as TTA/ nC_{60} . In this case, even a C_{60} concentration of 0.002 M can be reached [182]; the procedure was subsequently reconsidered [183]. Dilution of tetrahydrofuran solution of fullerene with water leads to hydrosols of THF/ nC_{60} type [184,185]. First, a fullerene

solution in THF is prepared in inert atmosphere, and after mixing with water the organic solvent is evaporated [184]. Dilution of C_{60} and C_{70} solutions in polar solvents *N*-methylpyrrolidine-2-one and dimethylformamide with water results in NMP/ nC_{60} , NMP/ nC_{70} [186], and DMF/ nC_{60} [155] colloidal systems. New versions of such approaches were developed by the Ausman group [183,187]. These authors proposed a new procedure using C_{60} solution in hexane, diluted with *iso*-propanol and water [187]; under such conditions, hexane is evaporated first.

An approach based on the introduction of a surfactant sodium dodecylsulfate (SDS) has been proposed. A fullerene solution in a “good” solvent is added to aqueous acetone containing SDS, and organic solvents are removed by distillation [188–190]. Here, SDS stabilizes the final C_{60} colloidal particles; however, utilization of surfactants, polymers, etc., is beyond the shape of this minireview.

Another “bottom-up” method was already reported as early as 1997. It consists of the introduction of THF solutions of the C_{60} anion radical into water; oxidation with atmospheric oxygen results in formation of a hydrosol [191]. This procedure was revisited after two decades [192]. Reaction with KOH and oxidation results in formation of fulleranol; the NIR spectra of fullerene anion radical and the properties of hydrosol of fulleranol is recently reported [193].

Preparation of colloid solutions can be performed using sonication. Solutions of C_{60} were prepared in DMF and THF by stirring and then, instead of mixing with water, the latter was added and accompanied with sonication only after the organic solvents evaporation [156]. The authors of the original article designate thus obtained as DMF/ nC_{60} and THF/ nC_{60} [156]. A versatile analysis of these obtained systems disclosed substantial chemical changes of the fullerene. Not only sonication but the nature of the organic solvent plays a role in these alterations [156].

More popular is the sonication method consisting in ultrasonic extraction from toluene to water [194]. The hydrosols prepared in this “bottom-up” way are designated as son/ nC_{60} , or tol/ nC_{60} , or SON/ nC_{60} . Contrary to the above mentioned procedures this allows to receive much higher fullerene concentrations, up to 0.001 M [195] and particle size down to 20 nm [16].

This method works well not only for C_{60} , but also for C_{70} [196–198] and C_{76} , C_{84} [196], and is permanently modified [196,199–203]. So, if the pH of the water phase is elevated to 10, the negative charge of the colloidal particles increases, therefore making them more stable [199]. Also, SDS was added in order to stabilize the particles that appear during the ultrasound extraction; the surfactant was removed from the final colloid via dialysis [203]. Some authors added small amounts of ethanol to the aqueous phase [196,200,204]. Slight heating to 40 °C and passing nitrogen to remove toluene traces is proposed [200]. For the same purpose, 15 min boiling of the final hydrosol can be used [201]. Heating the system during the sonication process up to 60 °C allows substantially decrease the size of colloidal particles [202].

The disadvantages of the method include the occurrence of the (possible) fullerene oxidation and other chemical reactions under conditions of sonication. So, reactive oxygen species are readily formed such as superoxide ions, singlet oxygen, etc. [16]. Conversion of toluene into the benzoic acid and benzoate is also reported [205,206].

In 2022, two new approaches to the C_{60} hydrosols preparation were published [14,15]. Merland et al. modified the extraction/sonication method and developed an emulsification–evaporation process in the presence of an amphiphilic polymer. Instead of toluene, trichloromethane or carbon disulfide was used. Kop et al. [14] proposed a fullerene–curcumin antioxidant system. These authors prepared the C_{60} hydrosols by 9-fold dilution of a solution in NMP with water, followed by stirring, dialysis, and filtration through a 450 nm-pored filter. The sols were stabilized by Tween-80, polyvinyl pyrrolidone, cyclodextrin, and curcumin with different combinations.

As an example of a hydrosol of C_{70} , the results of our recent study are presented in Figures 8 and 9 [198]. This colloid system of son/ nC_{70} type was prepared by Dr.

Vladimir Klochkov using highly pure benzene instead of toluene. At the C_{70} concentration of 3.3×10^{-6} M and 25°C , the size of particles is 97 ± 3 nm (Figure 8) and $\zeta = -40 \pm 4$ mV [198].

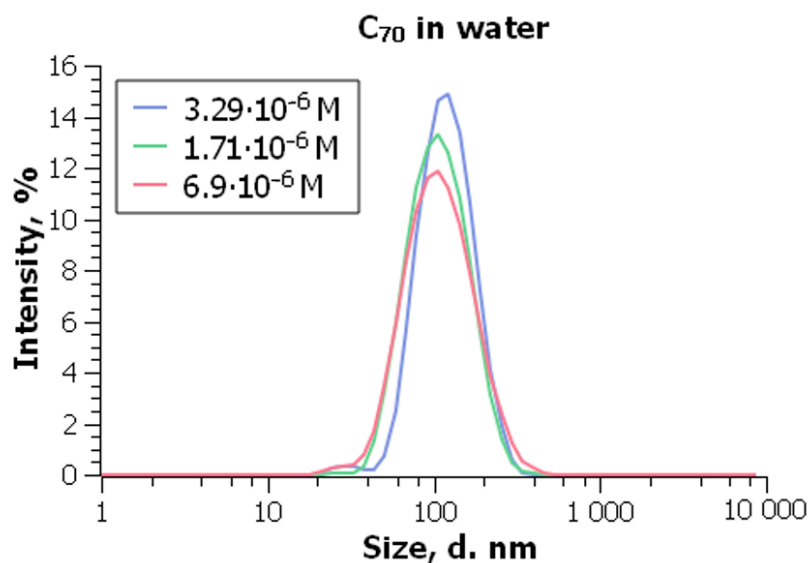


Figure 8. Particle size distribution in the son/ nC_{70} . From ref. [198] with permission.

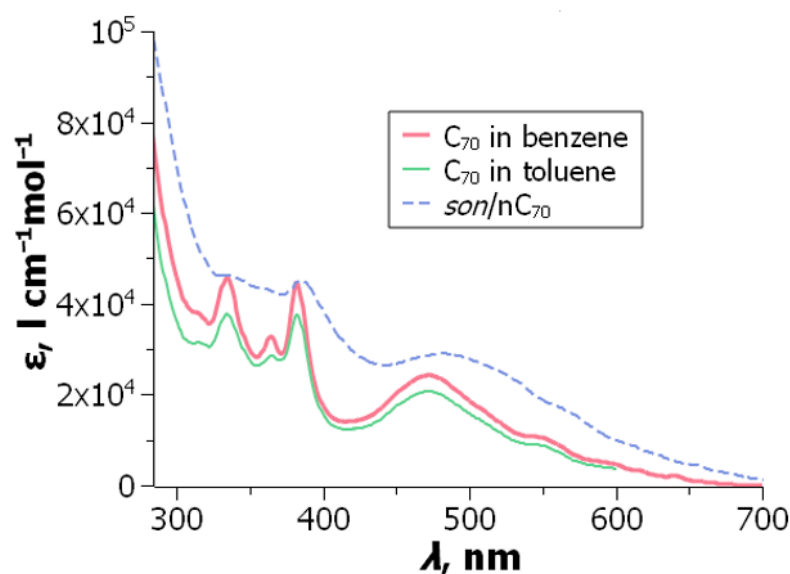


Figure 9. UV-visible absorption spectra of C_{70} in “good” solvents and in the son/ nC_{70} hydrosol. From ref. [198] with permission.

Increase in concentration displays insignificant alterations of the particle size; PDI is always around 0.2 [198]. The above characterization of this C_{70} hydrosol is in agreement with the results by Aich et al. [196].

The size/ ζ values for C_{70} hydrosols, available in the literature, as follows: 92 ± 14 nm/ -39 ± 4 mV [196]; 175 ± 5 nm/ -34.4 ± 0.7 mV [197]; ≈ 100 nm/ -21.7 mV [177] (in the last paper, the fullerene concentration was 8.9×10^{-5} M). As a rule, data are published without specifying the type of equation used for ζ calculation. As mentioned above, we used the Henry–Ohshima equation, which corresponds to the Hückel equation in the absence of foreign electrolytes.

It is important to note that relatively small variations in this preparation method often lead to formation of hydrosols with significantly different properties. This is a typical sign

of hydrophobicity of the colloidal system of interest. Given the widespread use of this method, it is important to try to standardize the synthetic protocol. Such attempts were made by Mikheev et al., who prepared standard samples of fullerene hydrosols [206,207]. Note that in these works as well in the study by Kyzyma et al. [186], sonication was used not only for the toluene–water system, but also during the preparation of the initial toluene solution of fullerenes. Contrary to it, we used to prepare the stock solutions in toluene and benzene without sonication, keeping the solid sample in the “good” solvent within ca. 2 weeks [198].

Finally, the “top-down” methods have been used, first of all, prolonged stirring of the solid samples of fullerene in water. Thus, the obtained colloid systems were designated as aq/nC_{60} , aq/nC_{60} , $stir/nC_{60}$, or STI/nC_{60} . Sometimes stirring continued even 1075 days [208]. Murdianti et al. [209] presented experimental evidence that suspension formation does not occur in an inert atmosphere. They attach a key importance to the formation of fullerene oxide $C_{60}O$ for the appearance of colloidal particles [209]. Based on detailed studies, it was concluded that it is impossible to obtain identical results by mixing in water [210].

Mixing and stirring can be performed in the presence of salts of organic acids. For example, if citrate is used, the colloid is named as cit/nC_{60} [211]. Some authors used sonication in water and named the colloid as $aq/SON/nC_{60}$ [210], while others crushed a solid fullerene sample in water by a laser beam [212]. The hand-grinding of the solid sample in a mortar followed by transfer to water and sonication was named mechano-assisted reduction of size, or $MARS/nC_{60}$ [213,214], is preferably carried out on with the addition of SDS [25]. In any case, filtration of the resulting colloid solutions using 220 or 450 nm pore filter is highly recommended.

4.5. Hydrosols of Fullerenes: Key Properties

Briefly summarizing the numerous data accumulated to date, we can give the following characteristics of hydrosols or suspensions of fullerenes. These are typical hydrophobic colloidal nanodispersed systems, with the size of negatively charged particles being between ≈ 40 and ≈ 200 nm, and with fullerene concentration, as a rule, below 0.01 mass %. Although it is obvious that the authors of various works sought to obtain the maximum concentration of fullerene, the final concentrations depend to a large extent on the method of preparation used. Other properties of the colloids also strongly depend on the preparation protocol. Such scattering of the properties of the colloidal solutions prepared by different methods or even by the same methods but by different authors gives additional support to the idea of pronounced hydrophobic character of the systems of interest.

Since the initial weight of fullerene usually cannot be completely transferred into water, it is necessary to have a method for determining the fullerene concentration in solution. A common method consists of deposition of fullerene colloidal species by $Mg(ClO_4)_2$, $NaCl$, $NaNO_3$ or/and acetic acid followed by extraction with toluene and absorbance measurements [24,25,183,187]. New method basing on the light scattering has also been developed [210].

As for the determination of particle size and polydispersity of fullerene aqueous dispersions, the dynamic light scattering method is used first of all. However, indirect methods based on UV-visible absorption spectra [213,215,216] may also be used. For example, Deguchi et al. [213] proposed an equation that describes the dependence of the absorption maximum in the region of 340–350 nm on the hydrodynamic diameter of the colloidal particle determined using the DLS method, Equation (1).

$$\lambda_{\max} = (337.1 \pm 1.4) + (0.065 \pm 0.009) d_H \quad (1)$$

The discussion of applicability of this and other equations can be found in a previous review [25]. A more detailed characterization provides for knowledge about impurities, first of all oxidation products [156,183,187,206,209].

The origin of the negative charge of the colloidal particles is of special interest because it allows to shed additional light on the nature of the fullerene/water interface. Several popular explanations of the charge origin have been considered and discussed in previous reviews [24,25]. The most probable reasons are as follows. (i) Adsorption of the HO^- ions, which is typical for many hydrophobic surfaces such as oil droplets [217] and gas bubbles [218]. (ii) Localized hydrolysis caused by electrophilic properties of fullerenes, which are in fact Lewis acids [24,25,219]; it also favors the additional formation of the HO^- ions. The role of HO^- ions in formation of the surface charge is supported both by additional stabilization at pH above 7 and coagulation at pH 1–2 [25]. (iii) Quantum-chemical calculations made by Choi et al. [220] revealed that the interactions between fullerene and water molecules lead to charge transfer and polarization, thus making a contribution to the negative charging of the fullerene aggregates in water. This explanation is in line with our concept (ii).

In any case, the negative charge is a main factor of the aggregative stability of colloids including fullerene sols and suspensions. Noneman et al. [221] performed a detailed molecular dynamics modeling of mixtures of C_{60} with C_{60}O in water. The main idea of this and of previous works of this group [183,187,209] consists of stabilization of C_{60} colloids in water by admixtures of C_{60}O . The latter to some extent plays the role of a diphilic compound, a kind of stabilizing surfactant [221]. This is quite plausible, but the fullerene oxide itself cannot cause the surface charge, and it is the charge screening by electrolytes that leads to coagulation.

According to molecular simulations made by Hinkle and Phelan [222], the Gibbs solvation energy, ΔG_{solv} , of C_{60} in water ($-50.9 \text{ kJ mol}^{-1}$) is more negative than that reported by Stukalin et al. [93]. However, the energy of transfer from water to methanol and ethanol is -68.1 and $-86.5 \text{ kJ mol}^{-1}$, respectively. The ΔS_{solv} value of C_{60} hydration is negative. These parameters, however, refer to the C_{60} molecule and not to the colloidal particle. Voronin et al. [223] estimated the negative entropic ΔS value by studying a son/ $n\text{C}_{60}$ hydrosol using DLS method at different temperatures, atomic force microscopy, and isothermal titration calorimetry. Based on the combined equation of the first and second laws of thermodynamics, they stated that the C_{60} fullerene aggregation in aqueous solution is entropically driven, occurring with nearly zero enthalpy change. However, the use of a thermodynamic approach for a hydrophobic colloidal system is clearly inappropriate.

Recently, Godínez-Pastor and González-Melchor [224] published a detailed molecular dynamics study of the behavior of the fullerene/water system under liquid and liquid–vapor conditions. A computational study of fullerene/water systems under liquid phase and liquid-vapor conditions was performed using atomistic model. At 300 K and 1 bar, fullerene aggregates were observed. The aggregation was less defined at 373 K and 10 to 24 kbar [224].

In addition to the hydrosols and aqueous suspensions of fullerenes, the C_{60} layers on the water/air interface should be mentioned. Kolker and Borovkov [225] used cyclohexane as spreading solvent and prepared a diluted highly homogeneous 2D system $\text{C}_{60}\text{--H}_2\text{O}$. They also showed that under compression, instead of true Langmuir monolayers, polylayers up to hexalayers can arise. This system can be considered as an interfacial colloid system; the cited article also provides a review of the relevant literature data [225].

Another interesting issue is the partition of fullerenes between water and nonpolar solvents. Mikheev et al. [226] presented a detailed quantitative study of partition of C_{60} and C_{70} between mutually saturated water and toluene. The specificity of their approach consists of using sonication; the ratio of concentration of fullerenes in aqueous and organic phases was relatively similar when the quasi-equilibrium state was reached from both sides. The distribution constants for the two fullerenes were found to be 6 and 2, respectively [226]. Note that Jafvert and Kulkarni [227] determined the partition constants of C_{60} between toluene or 1-octanol and water, 2.8×10^8 and 4.7×10^6 , respectively. These values for mutually saturated solvents were obtained using three different procedures and describe the equilibrium of single C_{60} molecules in different solvents. The solubility of fullerene

in water was estimated as 1×10^{-11} M [227]. Such difference of partition constants is understandable because in the first paper [226], fullerene is in colloid state in water and, probably, in toluene under conditions of sonication.

This problem is to some extent connected with the partition of nanoparticles between water and organic solvents, including 1-octanol [228]. The last concept was criticized by Praetorius et al. [229], because, for lyophobic systems, the thermodynamic approach is not correct. Their paper is entitled “The road to nowhere: equilibrium partition coefficients for nanoparticles” [229]. Based on an approach developed by Hill [230], Shchukin et al. [231] mentioned that a disperse system with very small particles can be conditionally regarded as a one-phase colloidal solution containing large “molecules”. However, for the partition of charged particles of a lyophobic system between two liquid phases it can be really misleading.

The colloidal particles, including those of fullerenes in water are charged, which hinders their transfer into the organic phase. However, Mikheev et al. [226] explained their results by transferring of single molecules. They estimated a maximum concentration of C_{60} in water produced from a toluene solution by the solvent-exchange procedure, i.e., in the son/n C_{60} sol, as 5.6×10^{-4} M. Though their results are self-consistent, it would be worthwhile to process the experiments using other parameters of sonication. For example, Scharff et al. managed to prepare a son/n C_{60} colloid with concentration of 1.9×10^{-3} M [232].

5. Coagulation by Electrolytes

5.1. Coagulation of Hydrosols and Aqueous Suspensions

Hydrosols of C_{60} and C_{70} are typical lyophobic colloidal systems with negatively charged particles [20,22–25,198,229,233,234]. They readily coagulate on adding electrolytes, are irreversible (i.e., cannot be spontaneously restored after the complete evaporation of the solvent), and exhibit the so-called coagulation zones, i.e., coagulation—stabilization—coagulation, in the presence of cationic surfactants [16,25,198,233]. The particle size, size distribution, electrokinetic potential, and other properties for fullerene hydrosols and suspensions prepared by different methods and by different authors do not coincide. This is typical for lyophobic (hydrophobic) systems. As a result, a pronounced scatter of the critical coagulation concentrations, CCC, becomes evident after gathering numerous results available in the literature [25]. So, the reported CCC for NaCl vary from 25 mM [203] to 321 [235]. Some representative examples are given in Figure 10 and Table 4.

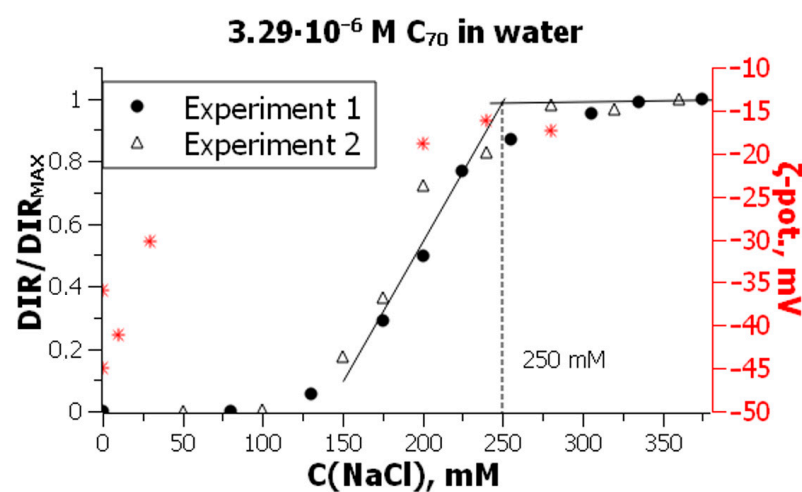


Figure 10. Determination of the critical coagulation concentration of the C_{70} hydrosol by NaCl: the results of two independent experiments; DIR is the diameter increase rate; asterisks indicate the ζ values. From ref. [198] with permission.

Table 4. The critical coagulation concentrations of fullerene hydrosols by electrolytes ^a.

Type of Hydrosol	Fullerene Conc., M	CCC, mM			CCC(NaCl): CCC(CaCl ₂)	Ref.
		NaCl	CaCl ₂	LaCl ₃ , La(NO ₃) ₃		
son/nC ₆₀	1 × 10 ⁻⁴	85	4.1	0.056	21	[233]
son/nC ₆₀	1.5 × 10 ⁻⁵	140	—	—	—	^b
son/nC ₆₀	3.9 × 10 ⁻⁵	321	6.7	—	48	[235]
son/nC ₆₀	8.2 × 10 ⁻⁶	160	6.1	—	26	[236]
son/nC ₆₀	9.2 × 10 ⁻⁷	220	10	—	22	[237]
son/nC ₇₀	3.3 × 10 ⁻⁶	250	—	0.070 ^b	—	[198]
son/nC ₇₀	1.7 × 10 ⁻⁵	145	—	—	—	[198]
son/nC ₇₀	6.9 × 10 ⁻⁵	130	—	—	—	[198]
son/nC ₇₀	7.9 × 10 ⁻⁷	150	12	—	12	[237]
son/nC ₇₆	7.3 × 10 ⁻⁶	100	6	—	17	[237]
son/nC ₈₄	6.6 × 10 ⁻⁶	70	7.5	—	9	[237]
aqu/nC ₆₀	1.1 × 10 ⁻⁵	140	5.3	0.11	26	[238]
aqu/nC ₆₀	4.2 × 10 ⁻⁶	295	5.9	—	50	[235]
aqu/nC ₆₀	1.5 × 10 ⁻⁶	84	4.25	—	20	[239]
THF/nC ₆₀	9.7 × 10 ⁻⁶	104	4.8	—	22	[17]

^a A much larger body of data can be found in ref. [25]. ^b Our data, to be published.

A theoretical study by Mortuza et al. [122] sheds additional light on the electrolyte-induced coagulation of fullerene hydrosol. In the first paper [120], it was demonstrated by molecular dynamics simulation that uncharged fullerenes aggregate in water, the charged species avoid it because of electrostatic repulsion. In the second study [122], the increase in the size of the C₆₀ clusters in the 100 mM NaCl solution was described using a combination of molecular dynamics and kinetic Monte Carlo method. The mechanism of cluster growth turns in salt solutions from the reaction limited to the diffusion limited cluster aggregation (RLCA → DLCA) [122].

The most regularities of coagulation were described in outline as early as 1997 [233]. Before that in the same year, it was mentioned that a C₆₀ sol, obtained by oxidation of fullerene anion-radical, can be precipitated using NaOH, HCl, NaCl, and BaCl₂ [191]. Since then, many studies have been performed using more advanced methods for CCC determinations [198,235–242]. Using the DLS method, Meng et al. [242] determined CCC = 98 mM for NaCl at 1.39 × 10⁻⁵ M C₆₀ solutions; Khokhryakov et al. [243] obtained a CCC value of 100 mM for C₆₀ concentration of 4.00 × 10⁻⁴ M using UV-visible spectra. (In Table 5 in ref. [25], for the last two articles the fullerene concentrations were indicated with an error.). In a study by Aich et al., the coagulation parameters of C₆₀, C₇₀, C₇₆, and C₈₄ colloids were determined [237].

For NaCl and KCl, a CCC of 167 mM is average of nineteen values [25]. In these studies performed by different authors, the fullerene concentrations varied from ~10⁻⁶ to ~10⁻⁴ M [25]. For salts with double-charged cations, CaCl₂, MgCl₂, and MgSO₄, an average value of 6.8 mM can be calculated using results of twenty-three studies [25]. This leads to a ratio of the averaged CCC values of single-charged to double-charged cations about 25. Importantly, despite the scatter of the results of different authors, the classical Schulze–Hardy rule is valid in the case of fullerene hydrosols.

For salts with a triple-charged cation, La³⁺, two reports are available for C₆₀ hydrosol. The ratio of reciprocal CCCs for Na⁺, Ca²⁺, and La³⁺ was determined as 1:21:1518 [233]. This result was subsequently confirmed by Zhang et al. [238]: 1:26:1272; such agreement is sufficient for lyophobic colloid systems. The DLVO theory in its classical version predicts the ratio of 1:64:729 (the so-called z⁶ law) for sols with highly charged particles and in the absence of ion adsorption [244]. Since then, a number of modifications of the theory were proposed [245–248], and this process is ongoing [249–251]. Among other problems, the role of the colloidal particles size [252], overcharging, hetero- and mutual coagulation [253–256], consideration of structural forces [257], and the role of the co-ions (or

similiions) influence [258] are discussed in order to refine the theory. For a long ago studied hydrosol As_2S_3 , an example of the above ratio for single-, double-, and triple-charged cations is 1:80:725, whereas for AgI hydrosol, it is 1:58:2029. These are averaged values from a fundamental book [259].

For relative to fullerenes nanocarbon systems, single- and multi-walled nanotubes, SWCNT, and MWCNT, respectively, with different degrees of oxidation, twenty-nine CCC values for NaCl, thirty-two CCC values for calcium, magnesium, and barium salts, and five CCC values for cerium, lanthanum, and aluminum salts give an averaged ration of coagulative power: 1:71:2775 [260]. For a sample of SWCNT with 10 mass % oxygen, studied by us, the CCCs for NaCl, $\text{Ca}(\text{Ba})\text{Cl}_2$, and $\text{La}(\text{NO}_3)_3$ are 150; 1.4; and 0.025 mM, which corresponds to the CCC^{-1} ratio 1:107:6000 [260]. Specific interactions with oxygen-containing groups, obviously carboxylic, take place for multi-charged metal cations. Either blocking the carboxylic groups by methylation or decarboxylation results in drop of the $\text{CCC}(\text{NaCl})/\text{CCC}(\text{Ca}(\text{Ba})\text{Cl}_2)$ ratio by an order of magnitude [260].

Two works connected with the fullerene–electrolyte interaction under unusual conditions should be mentioned. First, the state of C_{60} layers on the water/air interface is affected by introducing 1% (i.e., 171 mM) of NaCl. The hydrophobic hydration is hindered, and the sub-monolayer structure becomes cross-linked due to direct contacts between fullerene molecules [225]. Note that the above NaCl concentration is around the CCC value of hydrosols. It should be kept in mind that coagulation in the interfacial layers and even the 2D Schulze–Hardy rule is described in the literature [261].

Second, Gigault et al. [178] revealed using in situ DLS, that $n\text{C}_{60}$ aggregation on passing the salinity gradient in a micro-fluid occurs not so expresses as under common bulk conditions at the same NaCl concentrations.

For the same colloidal system, the CCC value sometimes depends on the sol concentration. An increase in the CCC value for a single-charged coagulating ion of the electrolyte along with the dilution of the sol is known as the Burton–Bishop rule [262–264], which would be more accurately called the Mukherjee–Sen–Burton–Bishop rule [265]. For some colloidal systems, it was not confirmed [263,264], but it works for fullerene hydrosols. Whereas the particle size of C_{70} hydrosol stays practically unaffected at the fullerene concentration within the range of 3.3×10^{-6} to 6.9×10^{-5} M, the CCC value drops from 250 to 130 mM NaCl [198]. This finding resembles the same effect for C_{60} [25].

The behavior of fullerene hydrosols in the presence of a cationic surfactant is well within the classical principles of colloid chemistry [264,266]. For the C_{70} hydrosol at 3.3×10^{-6} M, the $\text{CCC} = 0.005$ mM value for CTAB is fifty thousand times lower than for NaCl [198]. A jump in size from ca. 100 nm up to ca. 550 nm and substantial decrease in $|\zeta|$ is observed. At higher CTAB concentrations, overcharging takes place up to $\zeta = +40$ mV at surfactant concentration of 0.02 mM. Both effects occur well below the critical micelle concentration of CTAB, 0.9 mM, and are certainly caused by the surfactant adsorption: first layer of CTA^+ neutralizes the surface charge and leads to the hydrophobization of the surface of colloid particles, while the second, tail-to-tail layer, results in overcharging and stabilization of the particles. This is in line with the results earlier obtained with C_{60} [16]. Such “coagulation zones” were observed for the Au, As_2S_3 , AgI hydrosols with a number of cationic surfactants [264,266], and SiO_2 –CTAB system [267]. The peculiarity of the systems of interest is the extremely low concentration of fullerenes, contrary to much higher concentration of the colloids in the above cited works [259,262–264].

The coagulation data can be explained in terms of the universally recognized DLVO theory. However, the exact value of the Hamaker constant for fullerene–fullerene interaction, A_{FF} , stays unknown. So, an attempt might be done to solve the inverse problem. In this case, an A_{FF} value corresponding to the CCC value, particle size, and electrical surface potential should be regarded the most reliable. In the classical version, the DLVO approach considers only two contributions to the energy of interaction between two col-

loidal particles, U , the energies of electrostatic repulsion, U_{el} , and molecular attraction, U_{mol} , Equation (2).

$$U = U_{el} + U_{attr} \quad (2)$$

We used the Dukhin – Derjaguin – Semnikhin version [245] of the DLVO theory, Equation (3).

$$U = U_{el} + U_{attr} = 64\pi\epsilon_r\epsilon_0 \left(\frac{RT}{F}\right)^2 \operatorname{tgh}^2\left(\frac{\Psi_d F}{4RT}\right) \frac{r \exp(-\kappa h)}{s} - \frac{A_{FSF}^*}{6} \left[\frac{2}{s^2 - 4} + \frac{2}{s^2} + \ln \frac{s^2 - 4}{s^2} \right] \quad (3)$$

Here, h stands for the distance between the centers of the particles, $s = 2 + h/r$, $\epsilon_0 = 8.854 \times 10^{-12} \text{ F m}^{-1}$, κ is the reciprocal Debye length, R , T , F have their usual meanings, Ψ_d is the electrical potential of outer Helmholtz plane; usually, the experimentally available ζ value is used instead of Ψ_d , which is a kind of a Galvani potential.

The A_{FSF}^* value characterizes the fullerene–solvent–fullerene interaction in solution. It is connected with the A_{FF} and A_{SS} values, which characterize the fullerene–fullerene and solvent–solvent interaction in vacuum, through the Hamaker equation:

$$A_{FSF}^* = (A_{FF}^{1/2} - A_{SS}^{1/2})^2 \quad (4)$$

The Hamaker diagrams, i.e., the dependences of U on h , can be constructed. Various A_{FSF}^* values can be used, and those that met the coagulation conditions were selected. Then, Equation (4) should be used to estimate the A_{FF} value. The systems with $U_{\max} \approx (0-2)k_B T$ can be considered as unstable and corresponding to the experimentally determined CCC (k_B is the Boltzmann constant).

For C_{70} hydrosol, Figure 10, such an approach leads to $A_{FF} = 7.0$ and $6.2 \times 10^{-20} \text{ J}$ for $U_{\max} = 0$ to $1 k_B T$, respectively [198]. The results reported by the Elimelech group for the C_{60} hydrosol lead to an A_{FF} value of $7.5 \times 10^{-2} \text{ J}$ [240,241]. Our processing of the data of these authors leads to a value of $7.35 \times 10^{-20} \text{ J}$, though somewhat different versions of the DLVO theory were used [70]. The utilization of other results of the same research group [242] results in $A_{FF} = 5.25 \times 10^{-20} \text{ J}$ [70].

Although consideration of C_{60} (or C_{70})(OH) $_x$ fullerenols in water is beyond the scope of this review, two points should be noted. First, despite excellent solubility, fullerenols as a rule exist in water in form of aggregates [24]. Second, coagulation of fullerene in water takes place in diluted KCl solutions, despite the substantial initial negative ζ value of -60 mV [193]. It is obvious that the energy of molecular attraction is quite high due to the high surface atomic density of the fullerene structure.

5.2. Coagulation of Sols and Suspensions in Polar Organic Solvents (This Section Is Based Entirely on Experimental Results from This Laboratory [70,74,100,101,123,160])

Despite numerous studies devoted to fullerene colloidal solutions in polar and “good” + polar solvents, the stability of these systems in respect to electrolytes was not examined to the best of our knowledge. Accordingly, no information was available concerning the CCC values. On the contrary, many works on coagulation of aqueous colloidal fullerene solutions have been published. Obviously, this is due to the fact that both in biological systems and in environmental objects, the interaction of fullerenes with electrolytes is inevitable. But paradoxically, the study of the aggregative stability of organosols can shed additional light on the nature and properties of hydrosols.

The first experiments made by us have already shown that in polar organic solvents, the C_{60} aggregates readily coagulate and the CCC in acetonitrile-based solvents are two to three orders of magnitude lower than those in water [101]. For example, in acetonitrile with 1 vol.% toluene, the CCC value for NaClO_4 is 0.15 mM. Some representative values are collected in Table 5. The accuracy of the CCC values is normally around 15–20%.

Table 5. The CCC values of C₆₀ sols in different solvents, mM.

	In Water ^a	In Acetonitrile ^{b,c}	In Methanol ^{c,d}
Na ⁺	85 ^e	0.15–0.20	0.25–0.30
Ca ²⁺	4.1 ^f	0.016–0.030	0.04–0.05
La ³⁺	0.056	0.0068	—
H ⁺	0.55–1.2 ^g	0.14	0.3–1.0 ^h

Note. ^a From ref. [233]; metal cations were introduced in form of chlorides and nitrates. ^b From ref. [160]. ^c 1 vol.% toluene; metal cations were introduced as perchlorates. ^d From ref. [123]. ^e Average CCC of nineteen literary values is 167 mM (see Section 4.1). ^f Average CCC of twenty three literature values is 6.8 mM (see Section 4.1). ^g HClO₄, HCl, HNO₃. ^h The Fuchs curve for HClO₄ is unusually stretched.

The ratio of reciprocal CCC values for NaClO₄, Ca(ClO₄)₂, and La(ClO₄)₃ is 1:9:22. In an acetonitrile–benzene binary solvent, 1:1 by volume, the CCC values are higher due to incomplete dissociation of electrolytes [101]. In this case, the reciprocal CCC values are related as follows: 1 (NaClO₄):1.25 (HClO₄):2 (tetraalkylammonium perchlorates):9.1 {Ca(ClO₄)₂}:62.5 {La(ClO₄)₃}.

Other results obtained with C₆₀ and C₇₀ in methanol and acetonitrile (Figures 11 and 12, Table 6) confirm the above conclusions.

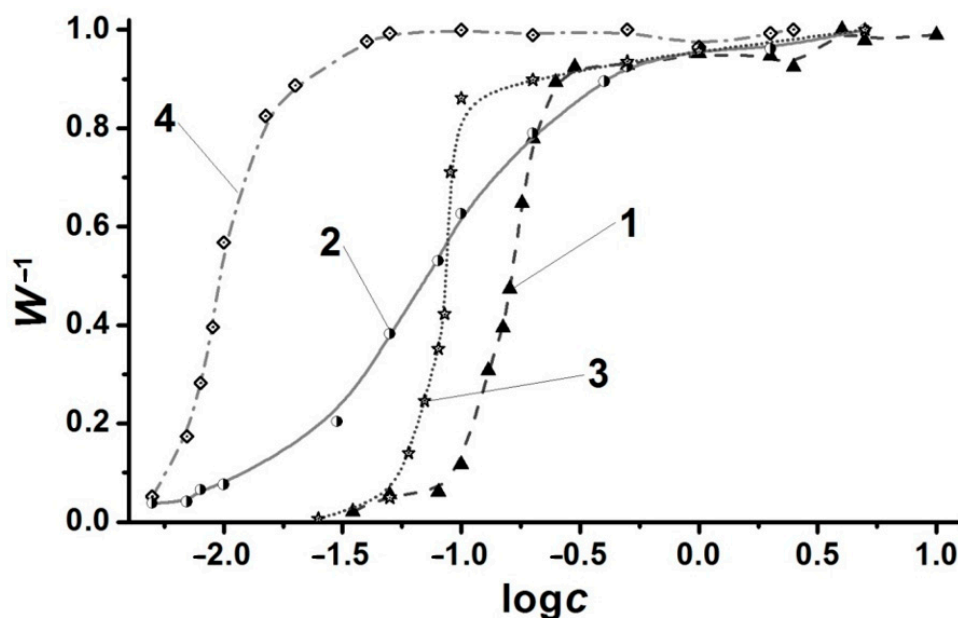


Figure 11. The reciprocal Fuchs function (= aggregation attachment efficiency) vs. logarithm of the electrolyte concentration (mM) in methanol: NaClO₄ (1); HClO₄ (2); TBAClO₄ (3); Ca(ClO₄)₂ (4). Reprinted from ref. [123] with permission.

Table 6. The CCC values of fullerene organosols with addition of 10 vol.% toluene, mM ^a.

	C ₇₀ in Acetonitrile	CCC(Na ⁺):CCC(Cation)	C ₆₀ in Acetonitrile	C ₇₀ in Methanol
Na ⁺	0.25	1	0.11	0.13
Li ⁺	0.024	10.4	0.02	0.13
H ⁺ ^b	0.015	16.7	0.15 ^c	—
Ca ²⁺	0.001	250	0.016–0.030 ^d	0.002
La ³⁺	0.0007	357	0.003 ^c ; 0.0068 ^d	—
Ca ²⁺	1.2 ^e	0.21	≈1 ^e	—

Note. ^a From ref. [70]. ^b Acids in organic solvents: perchloric, triflic, *p*-toluenesulfonic. ^c 6.6 vol.% benzene. ^d 1 vol.% toluene. ^e CCC₂.

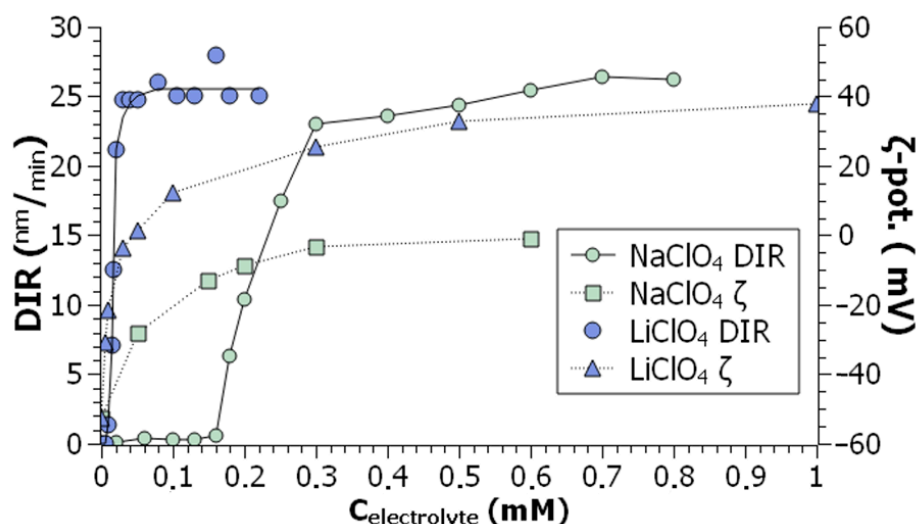


Figure 12. Diameter increase rate and ζ -potential of C_{70} particles (5×10^{-6} M C_{70}) in the presence of NaClO_4 or LiClO_4 in acetonitrile—toluene mixtures (10 vol.% toluene). From ref. [70] with permission.

Interestingly, in such systems, not only the Schulze–Hardy rule is valid but also the overcharging of colloidal particles by cations and appearance of “coagulation zones” takes place. The overcharging occurs at metal ion concentrations above the CCC and is very pronounced, for example, for C_{60} sols in acetonitrile with small additives of benzene or toluene, the electrokinetic potential increases from $\zeta = -(47\text{--}56)$ mV to $+(30\text{--}49)$ mV in the presence of Ca^{2+} , Ba^{2+} , and La^{3+} [101,160]. In methanol, the $\zeta = -37$ mV value increases up to $+37$ mV, $+26$ mV, and $+24$ mV for La^{3+} , Ca^{2+} , and Ba^{2+} , respectively [123]. The whole dependences of the electrokinetic potential on the electrolyte concentrations are available in the cited papers [123,160].

Such well-documented effects were not observed for the hydrosols [24,25,233]; the sole exception is a study of C_{60} in water in the presence of Al^{3+} ions [199]. The obvious reason for overcharging in organic solvent is, in addition to enhanced electrostatic interactions, poor solvation of the used cations in acetonitrile and methanol; the introduction of 18-crown-6 and cryptand [2.2.2] substantially weakens the effect due to binding of the metal cations into the macrocyclic ligand [101,123,160]. Even 10 mM *N*-cetylpyridinium perchlorate causes overcharging ($+11$ mV) [160]. Acids can also overcharge the colloidal particles in acetonitrile [101].

Such influence of adsorption on the coagulation process is in line with the observed deviation from the z^6 law. Experiments with C_{70} sols in acetonitrile were performed in the presence of 10 vol.% toluene; at lower content of the latter, the systems are less stable. The reciprocal CCC values for Na^+ , Ca^{2+} , and La^{3+} are given in Table 5. The overcharging of the initial colloidal C_{70} particles is very pronounced in acetonitrile: the values of $\zeta = -55$ mV to $+30$ mV in the presence La^{3+} and $+55$ mV for Ca^{2+} cations [70]. Even in LiClO_4 solutions the overcharging of particles reaches $+20$ mV [70].

The overcharging leads to an interesting phenomenon that is well documented for some colloidal systems studied long ago [253,254]. Namely, the appearance of the coagulation zones allows determining the second CCC value, or CCC_2 , corresponding to the coagulation of the modified, i.e., positively charged, fullerene aggregates [70,100,101,123,160]. This CCC_2 value for $\text{Ca}(\text{ClO}_4)_2$ is about 1.0 mM for C_{60} in acetonitrile with 1 vol.% toluene and 1.2 mM for C_{70} in the presence of 10 vol.% toluene (Table 6). Paradoxically, it is this CCC value that is better suited for estimating the Hamaker constant, which will be discussed below.

Another important issue is the low CCC value for LiClO_4 in acetonitrile, but not in methanol (Table 6). For C_{60} and C_{70} colloids, it is 5.5 and 10.4 times lower than that for NaClO_4 , respectively [70]. In concert with the pronounced overcharging in the case of

Li^+ this allows deducing that in the last case a typical heterocoagulation or even mutual coagulation takes place [254].

Moreover, the overcharging of colloidal particles by multi-charged counterions gives grounds to assume the effects of hetero- and mutual coagulation, which should affect the ratio of the CCC values [254].

First, the A_{FF} were estimated using the approach described above for hydrosols. Examples of the corresponding Hamaker diagrams are given in Figure 13. The values $(8.7\text{--}12.4) \times 10^{-20}$ J and $(6.6\text{--}13.7) \times 10^{-20}$ J were obtained in methanol [123] and acetonitrile [160], respectively. The first conclusion was as follows: these values are similar to the more precisely determined in water. However, more detailed analysis allowed selecting electrolytes that can be used in such reconstruction of the A_{FF} value [70]. The systems with pronounced change of the interfacial electrical potential due to adsorption of counterions were ruled out. In this case, higher A_{FF} values, such as 16×10^{-20} J (Table 7), are more probable and better agree with the high interfacial atomic density of fullerenes. The corresponding data for C_{60} are very similar.

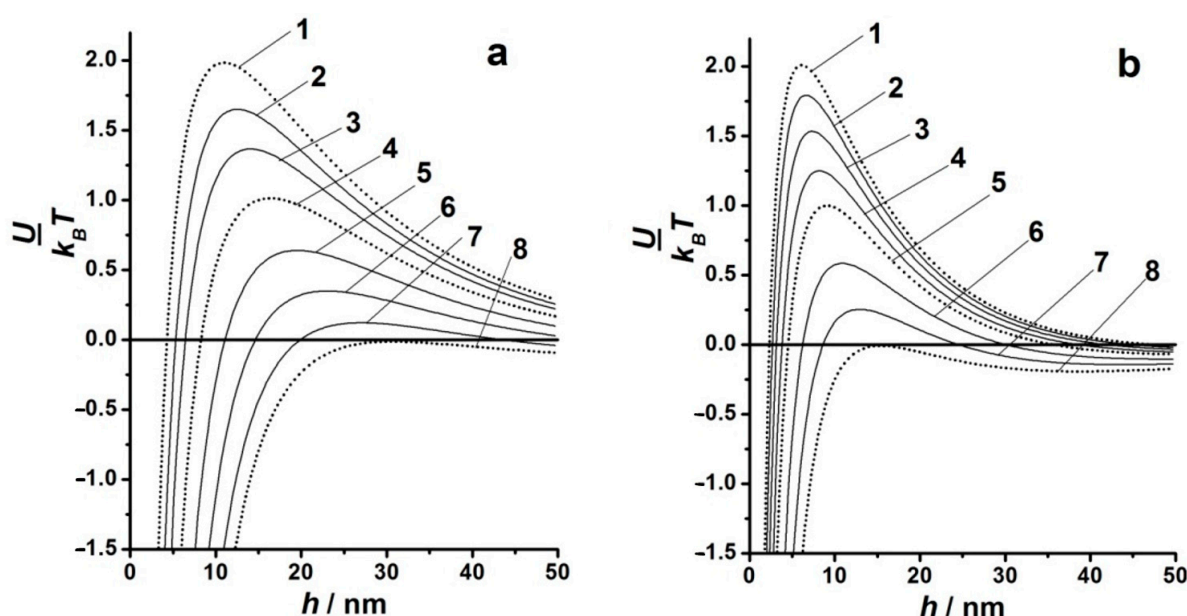


Figure 13. The Hamaker diagrams for C_{60} alcosol in methanol: (a)—for 0.10 mM ionic strength and $A^* \times 10^{20}$ J: 0.9 (1), 1.1 (2), 1.3 (3), 1.6 (4), 2.0 (5), 2.4 (6), 2.8 (7), 3.1 (8); (b)—for 0.30 mM ionic strength and $A^* \times 10^{20}$ J: 0.46 (1), 0.52 (2), 0.6 (3), 0.7 (4), 0.8 (5), 1.0 (6), 1.2 (7), 1.4 (8). The values $r = 150$ nm and $\zeta = -10$ mV are used in the constructing of the presented curves. From ref. [123] with permission.

Table 7. Examples of the A_{FF} estimation for C_{70} organosols ^a.

Salt	CCC, mM	ζ , mV	$A_{\text{FF}} \times 10^{20}$, J
NaClO_4	0.25	-6	5.8–8.0
$\text{Na}[2.2.2]\text{ClO}_4$	5.1	-15	7.7–7.9
$\text{Li}[2.2.2]\text{ClO}_4$	1.5	-20	11.8–13.2
$\text{N}(n\text{-C}_4\text{H}_9)_4\text{ClO}_4$	0.90	-21	14.5–16.0
$\text{Ca}(\text{ClO}_4)_2$	1.2	+40	16.2–16.6

Note. ^a C_{70} sols in acetonitrile with 10 vol.% toluene, 25 °C; radius of colloid particle: 150–160 nm; in the system with $\text{N}(n\text{-C}_4\text{H}_9)_4\text{ClO}_4$ —110 nm.

As a result, the A_{FF} value is substantially higher as compared to that estimated basing on coagulation of hydrosols. Accordingly, the construction of a Hamaker diagram for fullerene hydrosol using a higher Hamaker constant A_{FF} estimated in organosols, predicts the coagulation concentrations of electrolytes well below the experimental CCC (Figure 14).

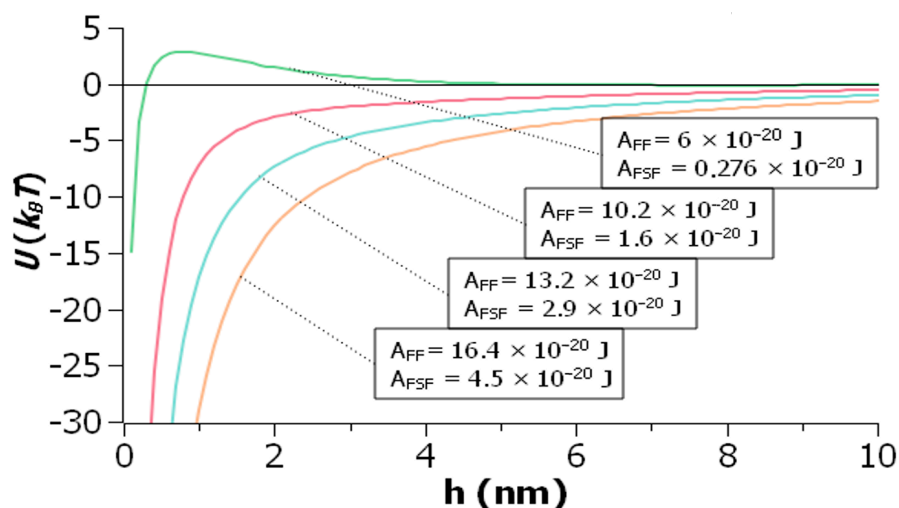


Figure 14. Hamaker diagrams for C_{60} hydrosol in 20 mM NaCl solution, $r = 44$ nm, $\zeta = -14.3$ mV constructed using different A_{FF} values. The upper (green) curve corresponds to the value $A_{FF} = 6.0 \times 10^{-20}$ J, which was obtained under assumption of the absence of any interactions except electrostatic repulsion and molecular attraction. From ref. [70] with permission.

These findings lead to an idea of some additional “non-DLVO” interactions in the hydrosols. According to the concept proposed long ago by Churaev and Derjaguin [257], a “structural” contribution, U_s , to the right hand side of Equation (2). The reason can be the specific interactions, for example described in ref. [220].

The idea of additional interactions “non-DLVO” in water, which are probably absent in acetonitrile, is convincingly supported by data for fullerene sols in DMSO and DMF [74]. In these cationophilic (protophilic) non-hydrogen bond donor solvents, the aggregative stability of fullerene sols increases dramatically. The Gutmann’s Donor Numbers (Table 2) for DMSO and DMF are with 29.8 and 26.6 much higher than those for acetonitrile (14.1) and methanol (19.1, conventional value). The value of the relative permittivity displays (if any) a secondary role; e.g., the ϵ_r values of acetonitrile and DMF is very close. This is clearly illustrated by the data for coagulation of the C_{70} sols with sodium salts in different solvents (Table 8).

Table 8. CCC values of $NaClO_4$ for C_{70} sols in different solvents ^a.

Solvent:	H ₂ O	CH ₃ OH ^c	CH ₃ CN ^c	DMSO
CCC, mM:	130–250 ^b	0.13	0.25	≥180

Note. ^a In water, NaCl was used. ^b Depending on the sol concentration. ^c With 10 vol.% toluene.

For instance, for the colloids of C_{70} in DMF and C_{60} in DMSO, the CCCs of $NaClO_4$ are 40 and 70 mM, respectively. This is ca. 200–300 times higher than in acetonitrile or methanol. For C_{70} in DMSO, the CCCs of $NaClO_4$ and $LiClO_4$ are no less than 180 mM. These abnormal values give evidence of substantial stabilizing factors, which is certainly caused by the basic character of DMSO and DMF and the electrophilic properties of fullerenes, which are Lewis acids. Note that in a basic (cationophilic) solvent, Li^+ ion is well solvated and displays no anomalous coagulating impact, contrary to the behavior in a cationophobic solvent acetonitrile.

In the case of $Ca(ClO_4)_2$ in DMSO, the negative charge of the C_{70} colloidal particles decreases substantially. This gives evidence for the pronounced role of adsorption of cations on the fullerene/DMSO interface. Nevertheless, the CCC value is with 1 mM 1000-fold higher than in acetonitrile.

Interestingly, *p*-toluenesulfonic acid acts pronouncedly in DMSO: for the sol C_{60} , CCC = 0.1 mM. Moreover, overcharging takes place and CCC₂ = 17 mM [74]. Hence,

even in DMSO, like in other solvents (water, acetonitrile, methanol), acidic medium is unfavorable for fullerene stability. The CCC values for acids in water, methanol, acetonitrile, and DMSO range from 1.2 to 0.015 mM (Tables 5 and 6).

Thus, despite the fact that fullerenes are Lewis acids, the negatively charged centers on the surface of colloidal particles have a basic character and are neutralized by protic acids, as well as by multiply charged metal cations, i.e., Lewis acids. A similar phenomenon was observed for oxidized single walled carbon nanotubes, SWCNT [268]. An aqueous suspension of SWCNT was five-fold diluted with acetonitrile, acetone, and alcohols, which decreases the CCC (NaCl) value by 1–2 orders of magnitude. In contrast, diluting the initial suspension with DMSO and DMF does not lead to a significant change in the CCC [268]. For organohydrosols of detonated nanodiamond, DND, with positive particle charge [269], the CCC values of most inorganic salts are higher than in water, if DMSO is the organic component, whereas in the mixtures of water with acetonitrile a pronounced drop of the CCC is observed. Here, the carbon atoms are in a state of sp^3 hybridization, but the strong solvation of DMSO particles is obviously due to the interaction of this cationophilic solvent with cationic centers on the DND surface.

Finally, Figure 15 reflects the pronounced increase in the stability of the C_{70} organosol with an increase in the DMSO: acetonitrile ratio.

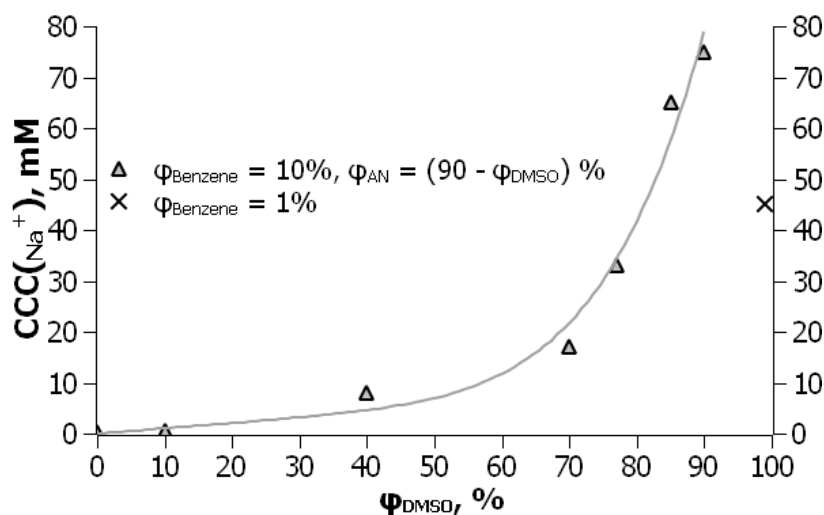


Figure 15. Dependence of the CCC($NaClO_4$) values of the C_{70} organosol on the volume fraction of DMSO in the ternary benzene–acetonitrile–DMSO system. From ref. [74] with permission.

Taking into account Table 2 and the behavior of fullerenes in NMP, considered in Section 4.2, the high stability of the corresponding organosols in respect to electrolytes can be predicted.

6. Conclusions

This review gives the following vision of the state of fullerenes in liquid media at the present time. In so-called “good” solvents, fullerenes exist in molecular form if the solutions are prepared by equilibrium methods. However, despite the molecular nature of such solutions, some of their properties resemble those of colloidal systems. The standard entropy of solvation and dissolution is significantly negative, while experiments prove that each fullerene molecule is surrounded by large solvation shells of an aromatic solvent. This makes the solution similar to systems known as colloidal crystals or periodic colloidal systems.

In polar or “poor” solvents such as acetonitrile or methanol, fullerenes form typical colloidal solutions with particle sizes up to several hundred nanometers. In binary “good” + “poor” solvent systems, the fullerene aggregates appear at a certain threshold solvent composition. The latter depends to some extent on the concentration of fullerene. It is

likely that C₆₀ and C₇₀ molecules are capable of retaining aromatic solvation shells even in colloidal aggregates.

A special group of polar solvents are NMP, DMSO, and DMF. These relatively basic solvents dissolve fullerenes without sonication. The solubility is higher than in other polar solvents, and large aggregates appear spontaneously. Formally, these solvents should be considered as “poor”, but with some features of “reactive” ones. Despite theoretical investigation of fullerenes in room temperature ionic liquids, the corresponding experimental data are few in number.

The interaction of fullerene hydrosols with electrolytes obeys all the classical laws and rules of colloid chemistry. There are known attempts to estimate the Hamaker constant of fullerene–fullerene interaction, A_{FF} , based on coagulation data. Two features of the behavior of C₆₀ and C₇₀ sols in acetonitrile and methanol fundamentally distinguish them from hydrosols. First, the critical concentrations of coagulations are two to three orders of magnitude lower than in water. Second, the overcharging of colloidal particles readily takes place. These phenomena make it difficult to process the data to estimate the Hamaker constant, A_{FF} , but after some judicious selection this value was found to be higher than that calculated from the hydrosol data. This allows us to derive some additional, non-DLVO specific interactions in water in accordance with the concept of “structural forces” by Churaev and Derjaguin.

The significance of specific interactions becomes obvious when studying the interaction of fullerenes with electrolytes in DMSO and DMF. In DMSO, the CCC is even higher than in water due to the strong solvation of fullerenes, which can be considered as Lewis acids.

Thus, in solvents of completely different chemical nature and physical properties, fullerenes can be obtained in a colloidal state. The systems discussed in this article provide many new illustrations for modern colloid chemistry.

Author Contributions: Conceptualization, N.O.M.-P.; methodology, N.O.M.-P., M.O.M. and N.N.K.; software, M.O.M. and N.N.K.; validation, N.O.M.-P., M.O.M. and N.N.K.; formal analysis, N.O.M.-P., M.O.M. and N.N.K.; investigation, N.O.M.-P., M.O.M. and N.N.K.; resources, N.O.M.-P.; data curation, N.O.M.-P., M.O.M. and N.N.K.; writing—original draft preparation, N.O.M.-P.; writing—review and editing, N.O.M.-P.; visualization, M.O.M. and N.N.K.; supervision, N.O.M.-P.; project administration, N.O.M.-P.; funding acquisition, N.O.M.-P. All authors have read and agreed to the published version of the manuscript.

Funding: This study was partially supported by the Ministry of Education and Science of Ukraine via grant number 0122U001485 and by the Simons Foundation (U.S.A.) via grant number 1030292.

Data Availability Statement: The data is available upon request.

Acknowledgments: N.O.M.-P. thanks the Shengzhou Mingjia Environmental Constructing Engineering Co., Ltd., Peoples’ Republic of China, for financial support.

Conflicts of Interest: The authors declare no conflict of interest.

References

1. Jia, Z.; Zhong, H.; Shen, J.; Yu, Z.; Tao, J.; Yin, S.; Liu, X.; Chen, S.; Yang, S.; Kong, W. Precursor formula engineering enabling high quality solution processed C₆₀ films for efficient and stable inverted perovskite solar cells. *Chem. Eng. J.* **2022**, *446*, 136897. [[CrossRef](#)]
2. Bernardo, G.; Melle-Franco, M.; Washington, A.L.; Dalglish, R.M.; Li, F.; Mendes, A.; Parnell, S.R. Different agglomeration properties of PC61BM and PC71BM in photovoltaic inks—A spin-echo SANS study. *RSC Adv.* **2020**, *10*, 4512–4520. [[CrossRef](#)] [[PubMed](#)]
3. Pascual, J.; Kosta, I.; Palacios-Lidon, E.; Chuvilin, A.; Grancini, G.; Nazeeruddin, M.K.; Grande, H.J.; Delgado, J.L.; Tena-Zaera, R. Co-solvent effect in the processing of the perovskite: Fullerene blend films for electron transport layer-free solar cells. *J. Phys. Chem. C* **2018**, *122*, 2512–2520. [[CrossRef](#)]
4. Bakhranov, S.A.; Makhmanov, U.K.; Aslonov, B.A. The synthesis of C₇₀ fullerene nanowhiskers using the evaporating drop method. *Condens. Matter* **2023**, *8*, 62. [[CrossRef](#)]

5. Zhelezny, V.; Khliyeva, O.; Lukianov, M.; Motovoy, I.; Ivchenko, D.; Faik, A.; Grosu, Y.; Nikulin, A.; Moreira, A.L. Thermodynamic properties of isobutane/mineral compressor oil and isobutane/mineral compressor oil/fullerenes C₆₀ solutions. *Int. J. Refrig.* **2019**, *106*, 153–162. [[CrossRef](#)]
6. Mikheev, I.V.; Sozarukova, M.M.; Izmailov, D.Y.; Kareev, I.E.; Proskurnina, E.V.; Proskurnin, M.A. Antioxidant potential of aqueous dispersions of fullerenes C₆₀, C₇₀, and Gd@C₈₂. *Internat. J. Mol. Sci.* **2021**, *22*, 5838. [[CrossRef](#)]
7. Meshcheriakov, A.A.; Iurev, G.O.; Luttsev, M.D.; Podolsky, N.E.; Ageev, S.V.; Petrov, A.V.; Vasina, L.V.; Solovtsova, I.L.; Sharoyko, V.V.; Murin, I.V.; et al. Physicochemical properties, biological activity and biocompatibility of water-soluble C₆₀-Hyp adduct. *Colloids Surf. B.* **2020**, *196*, 111338. [[CrossRef](#)]
8. Tomchuk, A.A.; Voitshenko, I.S.; Shershakova, N.N.; Andreev, S.M.; Turetskiy, E.A.; Khaitov, M.R.; Ivankov, O.I.; Tropin, T.V.; Tomchuk, O.V.; Avdeev, M.V. Comparative structural study of C₆₀-lysine and C₆₀-piperazine biocompatible aqueous solutions. *Fuller. Nanotub. Carbon Nanostruct.* **2022**, *30*, 27–35. [[CrossRef](#)]
9. Pikula, K.; Johari, S.A.; Golokhvast, K. Colloidal behavior and biodegradation of engineered carbon-based nanomaterials in aquatic environment. *Nanomaterials* **2022**, *12*, 4149. [[CrossRef](#)]
10. Wang, Z.; Wang, D.; Li, B.; Wang, J.; Li, T.; Zhang, M.; Huang, Y.; Shen, C. Detachment of fullerene nC₆₀ nanoparticles in saturated porous media under flow/stop-flow conditions: Column experiments and mechanistic explanations. *Environ. Pollut.* **2016**, *213*, 698–709. [[CrossRef](#)]
11. Adorinni, S.; Cringoli, M.C.; Perathoner, S.; Fornasiero, P.; Marchesan, S. Green approaches to carbon nanostructure-based biomaterials. *Appl. Sci.* **2021**, *11*, 2490. [[CrossRef](#)]
12. Mikheev, I.V.; Pirogova, M.O.; Usoltseva, L.O.; Uzhel, A.S.; Bolotnik, T.A.; Kareev, I.E.; Bubnov, V.P.; Lukonina, N.S.; Volkov, D.S.; Goryunkov, A.A.; et al. Green and rapid preparation of long-term stable aqueous dispersions of fullerenes and endohedral fullerenes: The pros and cons of an ultrasonic probe. *Ultrason. Sonochem.* **2021**, *73*, 105533. [[CrossRef](#)] [[PubMed](#)]
13. Di Giosia, M.; Bomans, P.H.H.; Bottoni, A.; Cantelli, A.; Falini, G.; Franchi, P.; Guarracino, G.; Friedrich, H.; Lucarini, M.; Paolucci, F.; et al. Proteins as supramolecular hosts for C₆₀: A true solution of C₆₀ in water. *Nanoscale* **2018**, *10*, 9908–9916. [[CrossRef](#)] [[PubMed](#)]
14. Kop, T.J.; Bjelaković, M.S.; Živković, L.; Žekić, A.; Milić, D.R. Stable colloidal dispersions of fullerene C₆₀, curcumin and C₆₀-curcumin in water as potential antioxidants. *Colloids Surf. A* **2022**, *648*, 129379. [[CrossRef](#)]
15. Merland, T.; Drou, C.; Legoupy, S.; Benyahia, L.; Schmutz, M.; Nicolai, T.; Chassenieux, C. Self-Assembly in water of C₆₀ fullerene into isotropic nanoparticles or nanoplatelets mediated by a cationic amphiphilic polymer. *J. Colloid Int. Sci.* **2022**, *624*, 537–545. [[CrossRef](#)] [[PubMed](#)]
16. Gigault, J.; Budzinski, H. Selection of an appropriate aqueous nano-fullerene (nC₆₀) preparation protocol for studying its environmental fate and behavior. *Trends Anal. Chem.* **2016**, *80*, 1–11. [[CrossRef](#)]
17. Kyzyma, O.A. Liquid systems with fullerenes in organic solvents and aqueous media. *Ukr. J. Phys.* **2020**, *65*, 761–767. [[CrossRef](#)]
18. Kyzyma, O.A.; Tomchuk, A.V.; Avdeev, M.V.; Tropin, T.V.; Aksenov, V.L.; Korobov, M.V. Structural researches of carbonic fluid nanosystems. *Ukr. J. Phys.* **2019**, *60*, 835. [[CrossRef](#)]
19. Kharissova, O.V.; Oliva Gonziález, C.M.; Kharisov, B.L. Solubilization and dispersion of carbon allotropes in water and non-aqueous solvents. *Industr. Eng. Chem. Res.* **2018**, *57*, 12624–12645. [[CrossRef](#)]
20. Shukla, N.C.; Huxtable, S.T. Fullerene suspensions. In *Handbook of Nanophysics: Clusters and Fullerenes*; Sattler, K.D., Ed.; Taylor & Francis Group: Boca Raton, FL, USA, 2010; pp. 40.1–40.10.
21. Avdeev, M.V.; Aksenov, V.L.; Tropin, T.V. Models of cluster formation in solutions of fullerenes. *Russ. J. Phys. Chem. A* **2010**, *84*, 1273–1283. [[CrossRef](#)]
22. Mchedlov-Petrosyan, N.O. Fullerene C₆₀ solutions: Colloid aspect. *Chem. Phys. Technol. Surf.* **2010**, *1*, 19–37. (In Russian)
23. Mchedlov-Petrosyan, N.O. Fullerenes in molecular liquids. Solution in “good” solvents: Another view. *J. Mol. Liq.* **2011**, *161*, 1–12. [[CrossRef](#)]
24. Mchedlov-Petrosyan, N.O. Fullerenes in liquid media: An unsettling intrusion into the solution chemistry. *Chem. Rev.* **2013**, *113*, 5149–5193. [[CrossRef](#)] [[PubMed](#)]
25. Mchedlov-Petrosyan, N.O. Fullerenes in aqueous media: A review. *Theor. Exper. Chem.* **2020**, *55*, 361–391. [[CrossRef](#)]
26. Sivaraman, N.; Dhamodaran, R.; Kaliappan, I.; Srinivasan, T.G.; Vasudeva Rao, P.R.; Matthews, C.K. Solubility of C₆₀ in organic solvents. *J. Org. Chem.* **1992**, *57*, 6077–6079. [[CrossRef](#)]
27. Sivaraman, N.; Dhamodaran, R.; Kaliappan, I.; Srinivasan, T.G.; Vasudeva Rao, P.R.; Matthews, C.K. Solubility of C₇₀ in organic solvents. *Fuller. Sci. Technol.* **1994**, *2*, 233–246. [[CrossRef](#)]
28. Ruoff, R.S.; Tse, D.; Malhorta, R.; Lorents, D.C. Solubility of fullerene C₆₀ in a variety of solvents. *J. Phys. Chem.* **1993**, *97*, 3379–3383. [[CrossRef](#)]
29. Heymann, D. Solubility of fullerenes C₆₀ and C₇₀ in seven normal alcohols and their deduced solubility in water. *Fuller. Sci. Technol.* **1996**, *4*, 509–515. [[CrossRef](#)]
30. Heymann, D. Solubility of C₆₀ in alcohols and alkanes. *Carbon* **1996**, *34*, 627–631. [[CrossRef](#)]
31. Tomiyama, T.; Uchiyama, S.; Shinohara, H. Solubility and partial specific volumes of C₆₀ and C₇₀. *Chem. Phys. Lett.* **1997**, *264*, 143–148. [[CrossRef](#)]
32. Scrivens, W.A.; Tour, J.M. Potent solvents for C₆₀ and their utility for the rapid acquisition of ¹³C NMR data for fullerenes. *J. Chem. Soc. Chem. Commun.* **1993**, 1207–1209. [[CrossRef](#)]

33. Semenov, K.N.; Charykov, N.A.; Arapov, O.V.; Keskinov, V.A.; Pyartman, A.K.; Gutenev, M.S.; Proskurina, O.V.; Matuzenko, M.Y. The solubility of C₇₀ in n-alkanols-1 C1-C11 over the temperature range 20–80 °C. *Russ. J. Phys. Chem. A* **2008**, *82*, 753–757. [[CrossRef](#)]
34. Semenov, K.N.; Charykov, N.A.; Alekseyev, N.I.; Arapov, O.V. Solubility of light fullerenes in styrene. *J. Chem. Eng. Data* **2009**, *54*, 756–761. [[CrossRef](#)]
35. Semenov, K.N.; Charykov, N.A.; Keskinov, V.A.; Piartman, A.K.; Blokhin, A.A.; Kopyrin, A.A. Solubility of light fullerenes in organic solvents. *J. Chem. Eng. Data* **2010**, *55*, 13–36. [[CrossRef](#)]
36. Semenov, I.A.; Sitnikov, D.N.; Romanovskiy, A.A.; Ulyanov, B.A. Solubility and equilibria in binary mixtures of methanol with n-pentane, n-hexane, and n-heptane. *Izv. Vusov. Khim. Khim. Technol.* **2012**, *55*, 39–42.
37. Törpe, A.; Belton, D.J. Improved spectrophotometric analysis of fullerenes C₆₀ and C₇₀ in high-solubility organic solvents. *Anal. Sci.* **2015**, *31*, 125–130. [[CrossRef](#)] [[PubMed](#)]
38. Hansen, C.M.; Smith, A.L. Using Hansen solubility parameters to correlate solubility of C₆₀ fullerene in organic solvents and in polymers. *Carbon* **2004**, *42*, 1591–1597. [[CrossRef](#)]
39. Ghosh, H.N.; Sapre, A.V.; Mittal, J.P. Aggregation of C₇₀ in solvent mixtures. *J. Phys. Chem.* **1996**, *100*, 9439–9443. [[CrossRef](#)]
40. Fujitsuka, M.; Kasai, H.; Masuhara, A.; Okada, S.; Oikawa, H.; Nakanishi, H.; Watanabe, A.; Ito, O. Laser flash photolysis study on photochemical and photophysical properties of C₆₀ fine particle. *Chem. Lett.* **1997**, *26*, 1211–1212. [[CrossRef](#)]
41. Rudalevige, T.; Francis, A.H.; Zand, R. Spectroscopic studies of fullerene aggregates. *J. Phys. Chem. A* **1998**, *102*, 9797–9802. [[CrossRef](#)]
42. Nath, S.; Pal, H.; Sapre, A.V. Effect of solvent polarity on the aggregation of C₆₀. *Chem. Phys. Lett.* **2008**, *327*, 143–148. [[CrossRef](#)]
43. Nath, S.; Pal, H.; Sapre, A.V. Effect of solvent polarity on the aggregation of fullerenes: A comparison between C₆₀ and C₇₀. *Chem. Phys. Lett.* **2002**, *360*, 422–428. [[CrossRef](#)]
44. Alargova, R.G.; Deguchi, S.; Tsujii, K. Stable colloidal dispersions of fullerenes in polar organic solvents. *J. Am. Chem. Soc.* **2001**, *123*, 10460–10467. [[CrossRef](#)] [[PubMed](#)]
45. Sun, Y.-P.; Bunker, C.E. C₇₀ in solvent mixtures. *Nature* **1993**, *365*, 398. [[CrossRef](#)]
46. Sun, Y.-P.; Bunker, C.E. Formation and properties of C₇₀ solidlike species in room-temperature solutions. *Chem. Mater.* **1994**, *6*, 578–580. [[CrossRef](#)]
47. Sun, Y.-P.; Ma, B.; Bunker, C.E.; Liu, B. All-carbon polymers (polyfullerenes) from photochemical reactions of fullerene clusters in room-temperature solvent mixtures. *J. Am. Chem. Soc.* **1995**, *117*, 12705–12711. [[CrossRef](#)]
48. Mized, S.; Tarabsheh, H.; Marji, D. A spectrophotometric study of the charge transfer complexation of [60]fullerene with some amines. *Jordan J. Chem.* **2007**, *2*, 145–153.
49. Kampe, K.-D.; Egger, N.; Vogel, M. Diamino and tetraamino derivatives of buckminsterfullerene C₆₀. *Angew. Chem. Int. Ed.* **1993**, *32*, 1174–1176. [[CrossRef](#)]
50. Talukdar, S.; Pradhan, P.; Banerji, A. Electron donor-acceptor interactions of C₆₀ with n- and π-donors: A rational approach towards its solubility. *Fuller. Sci. Technol.* **1997**, *5*, 547–557. [[CrossRef](#)]
51. Marcus, Y.; Smith, A.L.; Korobov, M.V.; Mirakyan, A.L.; Avramenko, N.V.; Stukalin, E.B. Solubility of C₆₀ fullerene. *J. Phys. Chem. B* **2001**, *105*, 2499–2506. [[CrossRef](#)]
52. Ruoff, R.S.; Malhotra, R.; Huestis, D.L.; Tse, D.S.; Lorents, D.C. Anomalous solubility behaviour of C₆₀. *Nature* **1993**, *362*, 140–141. [[CrossRef](#)]
53. Beck, M.T. Solubility and molecular state of C₆₀ and C₇₀ in solvents and solvent mixtures. *Pure Appl. Chem.* **1998**, *70*, 1881–1887. [[CrossRef](#)]
54. Ruelle, P.; Farina-Cuendet, A.; Kesselring, U.W. Changes of molar volume from solid to liquid and solution: The particular case of C₆₀. *J. Am. Chem. Soc.* **1996**, *118*, 1777–1784. [[CrossRef](#)]
55. Cataldo, F. On the solubility parameter of C₆₀ and higher fullerenes. *Fuller. Nanotub. Carbon Nanostruct.* **2009**, *17*, 79–84. [[CrossRef](#)]
56. Wang, C.I.; Hua, C.C.; Chen, S.A. Dynamic solvation shell and solubility of C₆₀ in organic solvents. *J. Phys. Chem. B* **2014**, *118*, 9964–9973. [[CrossRef](#)] [[PubMed](#)]
57. Wang, C.I.; Hua, C.C. Solubility of C₆₀ and PCBM in organic solvents. *J. Phys. Chem. B* **2015**, *119*, 14496–14504. [[CrossRef](#)] [[PubMed](#)]
58. Peerless, J.S.; Bowers, G.H.; Kwansa, A.L.; Yingling, Y.G. Fullerenes in aromatic solvents: Correlation between solvation-shell structure, solvate formation, and solubility. *J. Phys. Chem. B* **2015**, *119*, 15344–15352. [[CrossRef](#)]
59. Zhang, Y.; Wang, W.; Wang, Y.-B. The nature of the noncovalent interactions between fullerene C₆₀ and aromatic hydrocarbons. *Comput. Theor. Chem.* **2017**, *1122*, 34–39. [[CrossRef](#)]
60. Bokare, A.D.; Patnaik, A. C₆₀ aggregate structure and geometry in nonpolar o-xylene. *J. Phys. Chem. B* **2005**, *109*, 87–92. [[CrossRef](#)]
61. Patnaik, A.J. Structure and in self-organized C₆₀ fullerenes. *Nanosci. Nanotechnol.* **2007**, *7*, 1111–1150. [[CrossRef](#)]
62. Tropin, T.V.; Avdeev, M.V.; Aksenov, V.L. Small-angle neutron scattering data on C₆₀ clusters in weakly polar solutions of fullerenes. *Crystallogr. Rep.* **2007**, *52*, 483–486. [[CrossRef](#)]
63. Nath, S.; Pal, H.; Palit, D.K.; Sarpe, A.; Mittal, J.P. Aggregation of fullerene, C₆₀, in benzonitrile. *J. Phys. Chem. B* **1998**, *102*, 10158–10164. [[CrossRef](#)]
64. Wang, Y.-M.; Kamat, P.V.; Patterson, L.K. Aggregates of C₆₀ and C₇₀ formed at the gas-water interface and in DMSO/water mixed solvents. A spectral study. *J. Phys. Chem.* **1993**, *97*, 8793–8797. [[CrossRef](#)]

65. Pushkarova, Y.; Kholin, Y. A procedure for meaningful unsupervised clustering and its application for solvent classification. *Cent. Eur. J. Chem.* **2014**, *12*, 594–603. [[CrossRef](#)]
66. Török, V.G.; Lebedev, T.T.; Cser, L. Small-angle neutron-scattering study of anomalous C₆₀ clusterization in toluene. *Phys. Solid State* **2002**, *44*, 572–573. [[CrossRef](#)]
67. Aksenov, V.L.; Avdeev, M.V.; Tropin, T.V.; Priezhev, V.B.; Schmelzer, J.W.P. Cluster growth and dissolution of fullerenes in non-polar solvents. *J. Mol. Liq.* **2006**, *127*, 142–144. [[CrossRef](#)]
68. Chamberlain, T.W.; Popov, A.M.; Knizhnik, A.A.; Samoilo, G.E.; Khlobystov, A.N. The role of molecular clusters in the filling of carbon nanotubes. *ACS Nano* **2010**, *4*, 5203–5210. [[CrossRef](#)]
69. Dattani, R.; Gibson, K.F.; Few, S.; Borg, A.J.; DiMaggio, P.A.; Nelson, J.; Kazarian, S.G.; Cabral, J.T. Fullerene oxidation and clustering in solution induced by light. *J. Colloid Int. Sci.* **2015**, *446*, 24–30. [[CrossRef](#)]
70. Mchedlov-Petrosyan, N.O.; Marfunin, M.O. Formation, stability, and coagulation of fullerene organosols: C₇₀ in acetonitrile–toluene solutions and related systems. *Langmuir* **2021**, *37*, 7156–7166. [[CrossRef](#)]
71. Ahn, J.S.; Suzuki, K.; Iwasa, Y.; Otsuka, N.; Mitani, T. Photoluminescence of confined excitons in nanoscale C₆₀ clusters. *J. Lumin.* **1998**, *76–77*, 201–205. [[CrossRef](#)]
72. Yeo, S.J.; Pode, R.; Ahn, J.S.; Kim, H.M. Study on the size of fullerene C₆₀ aggregates in solution by photoluminescence and HRTEM measurements. *J. Korean Phys. Soc.* **2009**, *55*, 322–326. [[CrossRef](#)]
73. Mchedlov-Petrosyan, N.O.; Kamneva, N.N.; Al-Shuuchi, Y.T.M.; Marynin, A.I.; Shekhovtsov, S.V. The peculiar behavior of fullerene C₆₀ in mixtures of ‘good’ and polar solvents: Colloidal particles in the toluene–methanol mixtures and some other systems. *Colloids Surf. A* **2016**, *509*, 631–637. [[CrossRef](#)]
74. Mchedlov-Petrosyan, N.O.; Marfunin, M.O.; Tikhonov, V.A.; Shekhovtsov, S.V. Unexpected colloidal stability of fullerenes in dimethyl sulfoxide and related systems. *Langmuir* **2022**, *38*, 10000–10009. [[CrossRef](#)] [[PubMed](#)]
75. Sun, Y.-P.; Bunker, C.E.; Ma, B. Quantitative studies of ground and excited state charge transfer complexes of fullerenes with *N,N*-dimethylaniline and *N,N*-diethylaniline. *J. Am. Chem. Soc.* **1994**, *116*, 9692–9699. [[CrossRef](#)]
76. Gun’kin, I.F.; Loginova, N.Y. Effect of nature of organic solvent on the absorption spectrum of C₆₀ fullerene. *Russ. J. Gen. Chem.* **2006**, *76*, 1911–1913. [[CrossRef](#)]
77. Cataldo, F.; Iglesias-Groth, S.; Hafez, Y. On the molar extinction coefficients of the electronic absorption spectra of C₆₀ and C₇₀ fullerenes radical cation. *Eur. Chem. Bull.* **2013**, *2*, 1013–1018. [[CrossRef](#)]
78. Ying, Q.; Marecek, J.; Chu, B. Solution behavior of buckminsterfullerene (C₆₀) in benzene. *J. Chem. Phys.* **1994**, *101*, 2665–2672. [[CrossRef](#)]
79. Ying, Q.; Marecek, J.; Chu, B. Slow aggregation of buckminsterfullerene (C₆₀) in benzene solution. *Chem. Phys. Lett.* **1994**, *219*, 214–218. [[CrossRef](#)]
80. Bezmelnitsin, V.N.; Eletsii, A.V.; Stepanov, E.V. Cluster origin of fullerene solubility. *J. Phys. Chem.* **1994**, *98*, 6665–6667. [[CrossRef](#)]
81. Bezmelnitsin, V.N.; Eletsii, A.V.; Okun, M.V. Fullerenes in solutions. *Phys.-Uspekhi* **1998**, *41*, 1091–1114. [[CrossRef](#)]
82. Ginzburg, B.M.; Tuichiev, S. Variations in the structure of aromatic solvents under the influence of microadditives of the C₆₀ fullerene. *Crystallogr. Rep.* **2007**, *52*, 108–111. [[CrossRef](#)]
83. Ginzburg, B.M.; Tuichiev, S. Variations in the structure of aromatic solvents under the influence of dissolved fullerene C₇₀. *Crystallogr. Rep.* **2008**, *53*, 645–650. [[CrossRef](#)]
84. Ginzburg, B.M.; Tuichiev, S.; Yakimanskii, A.V. Supramolecular benzene structure and its changes under the action of dissolved fullerenes. *Crystallogr. Rep.* **2011**, *56*, 238–241. [[CrossRef](#)]
85. Ginzburg, B.M.; Tuichiev, S.; Shukhiev, S. Permittivity of low-concentration C₆₀ fullerene solutions in *p*-xylene. *Tech. Phys. Lett.* **2009**, *35*, 491–493. [[CrossRef](#)]
86. Ginzburg, B.M.; Tuichiev, S.; Tabarov, S.K. Effect of C₆₀ fullerene on the boiling point of its solutions in some aromatic solvents. *Russ. J. Appl. Chem.* **2009**, *82*, 387–390. [[CrossRef](#)]
87. Ginzburg, B.M.; Tuichiev, S. On the supermolecular structure of fullerene C₆₀ solutions. *J. Macromol. Sci. B* **2005**, *44*, 517–530. [[CrossRef](#)]
88. Ginzburg, B.M.; Tuichiev, S.; Rashidov, D.; Sodikov, F.H.; Tabarov, S.H.; Shepelevskii, A.A. Step-wise concentration influence of fullerenes C₆₀ and C₇₀ on the various parameters of condensed systems. *J. Macromol. Sci. B* **2015**, *54*, 533–543. [[CrossRef](#)]
89. Zhelezny, V.P.; Khanchych, K.Y.; Motovoy, I.V.; Nikulina, A.S. On the nonmonotonous behavior of the thermal properties of fullerene C₆₀/o-xylene solutions. *J. Mol. Liq.* **2021**, *338*, 116629. [[CrossRef](#)]
90. Amer, M.S.; Bennett, M.; Maguire, J.F. A Brillouin scattering study of C₆₀/toluene mixtures. *Chem. Phys. Lett.* **2008**, *457*, 329–331. [[CrossRef](#)]
91. Fritsch, S.; Junghans, C.; Kremer, K. Structure formation of toluene around C₆₀: Implementation of the adaptive resolution scheme (AdResS) into GROMACS. *J. Chem. Theor. Comput.* **2012**, *8*, 398–403. [[CrossRef](#)]
92. Li, M.M.; Wang, Y.-B.; Zhang, Y.; Wang, W. The nature of the noncovalent interactions between benzene and C₆₀ fullerene. *J. Phys. Chem. A* **2016**, *120*, 5766–5772. [[CrossRef](#)] [[PubMed](#)]
93. Stukalin, E.B.; Korobov, M.V.; Avramenko, N.V. Solvation free energies of the fullerenes C₆₀ and C₇₀ in the framework of polarizable continuum mode. *J. Phys. Chem. B* **2003**, *107*, 9692–9700. [[CrossRef](#)]
94. Korobov, M.V.; Mirakyan, A.L.; Avramenko, N.V.; Olofsson, G.; Smith, A.L.; Ruoff, R.S. Calorimetric studies of solvates of C₆₀ and C₇₀ with aromatic solvents. *J. Phys. Chem. B* **1999**, *103*, 1339–1346. [[CrossRef](#)]

95. Kolker, A.M.; Islamova, N.I.; Avramenko, N.V.; Kozlov, A.V. Thermodynamic properties of C₆₀ fullerene solutions in individual and mixed organic solvents. *J. Mol. Liq.* **2007**, *131*–132, 95–100. [[CrossRef](#)]
96. Kozlov, A.V.; Kolker, A.M.; Manin, N.G.; Islamova, N.I. Polythermal study of C₆₀ solubility in tetralin. *Mendeleev Commun.* **2007**, *17*, 362–363. [[CrossRef](#)]
97. Herbst, M.H.; Dias, G.H.M.; Magalhães, J.G.; Tôrres, R.B.; Volpe, P.L.O. Enthalpy of solution of fullerene [60] in some aromatic solvents. *J. Mol. Liq.* **2005**, *118*, 9–13. [[CrossRef](#)]
98. Mchedlov-Petrosyan, N.O.; Kamneva, N.N.; Al-Shuuchi, Y.T.M.; Marynin, A.I.; Zozulia, O.S. Formation and ageing of the fullerene C₆₀ colloids in polar organic solvents. *J. Mol. Liq.* **2017**, *235*, 98–103. [[CrossRef](#)]
99. Marfunin, N.A.; Mchedlov-Petrosyan, N.O. Behavior of fullerene C₇₀ in binary organic solvent mixtures as studied using UV-vis spectra and dynamic light scattering. *Kharkiv Univers. Bull. Chem. Ser.* **2019**, 77–87. [[CrossRef](#)]
100. Mchedlov-Petrosyan, N.O.; Al-Shuuchi, Y.T.M.; Kamneva, N.N.; Marynin, A.I.; Kryshtal, A.P. Properties of the fullerene C₆₀ colloid solutions in acetonitrile as prepared by Deguchi's hand-grinding method. *Kharkiv Univers. Bull. Chem. Ser.* **2015**, 5–11. [[CrossRef](#)]
101. Mchedlov-Petrosyan, N.O.; Kamneva, N.N.; Al-Shuuchi, Y.T.M.; Marynin, A.I.; Zozulia, O.S.; Kryshtal, A.P.; Klochkov, V.K.; Shekhovtsov, S.V. Towards better understanding of C₆₀ organosols. *Phys. Chem. Chem. Phys.* **2016**, *18*, 2517–2526. [[CrossRef](#)]
102. Dubois, D.; Moninot, G.; Kutner, W.; Jones, M.T.; Kadish, K.M. Electroreduction of Buckminsterfullerene, C₆₀, in aprotic solvents. Solvent, supporting electrolyte, and temperature effects. *J. Phys. Chem.* **1992**, *96*, 7137–7145. [[CrossRef](#)]
103. Efremov, I.F. *Periodic Colloidal Structures*; Khimiya: Leningrad, Russian, 1971; 190p. (In Russian)
104. Efremov, I.F.; Us'yarov, O.G. The long-range interaction between colloid and other particles and the formation of periodic colloid structures. *Russ. Chem. Rev.* **1976**, *45*, 435–453. [[CrossRef](#)]
105. Sonntag, H.; Strenge, K. *Coagulation Kinetics and Structure Formation*; Springer Science + Business Media: New York, NY, USA, 1987; 191p.
106. Bartlett, P.; Ottewill, R.H. A neutron scattering study of the structure of a bimodal colloidal crystal. *J. Chem. Phys.* **1992**, *96*, 3306–3318. [[CrossRef](#)]
107. Rugge, A.; Ford, W.T.; Tolbert, S.H. From a Colloidal Crystal to an Interconnected Colloidal Array: A Mechanism for a Spontaneous Rearrangement. *Langmuir* **2003**, *19*, 7852–7861. [[CrossRef](#)]
108. Ostwald, W. *Die Welt der vernachlässigten Dimensionen. Eine Einführung in die Kolloidchemie mit besonderer Berücksichtigung ihrer Anwendungen*; Theodor Steinkopf: Dresden, Germany, 1921; 253p.
109. von Weimarn, P.P. *Die Allgemeinheit des Kolloidzustandes*, 2nd ed.; Theodor Steinkopf: Dresden, Germany, 1925; 504p.
110. Garcia-Hernandez, D.A.; Cataldo, F.; Machado, A. Acenes adducts with C₇₀ fullerene: Anthracene, tetracene and pentacene. *Fuller. Nanotub. Carbon Nanostruct.* **2016**, *24*, 679–687. [[CrossRef](#)]
111. Zhang, X.; Li, X.-D. Solvent atmosphere controlled self-assembly of unmodified C₆₀: A facile approach for constructing various architectures. *Chin. Chem. Lett.* **2014**, *25*, 912–914. [[CrossRef](#)]
112. Guo, R.-H.; Hua, C.-C.; Lin, P.-C.; Wang, T.-Y.; Chen, S.-A. Mesoscale aggregation properties of C₆₀ in toluene and chlorobenzene. *Soft Matter* **2016**, *12*, 6300–6311. [[CrossRef](#)] [[PubMed](#)]
113. Makhmanov, U.; Ismailova, O.; Kokhkharov, A.; Zakhidov, E.; Bakhramov, S. Features of self-aggregation of C₆₀ molecules in toluene prepared by different methods. *Phys. Lett. A* **2016**, *380*, 2081–2084. [[CrossRef](#)]
114. Makhmanov, U.; Kokhkharov, A.; Bakhramov, S. Organic fractal nano-dimensional structures based on fullerene C₆₀. *Fuller. Nanotub. Carbon Nanostruct.* **2019**, *27*, 273–278. [[CrossRef](#)]
115. Makhmanov, U.K. Refractive and Electrophysical Properties of Dispersed Solutions of Fullerene C₆₀ in Binary Solvents. *J. Eng. Phys. Thermophys.* **2022**, *95*, 527–532. [[CrossRef](#)]
116. Makhmanov, U.K.; Esanov, S.A.; Sidigaliyev, D.T.; Musurmonov, K.N.; Aslonov, B.A.; Chuliev, T.A. Behavior of C₇₀ fullerene in a binary mixture of xylene and tetrahydrofuran. *Liquids* **2023**, *3*, 385–392. [[CrossRef](#)]
117. Peerless, J.S.; Bowers, G.H.; Kwansa, A.L.; Yingling, Y.G. Effect of C₆₀ adducts on the dynamic structure of aromatic solvation shells. *Chem. Phys. Lett.* **2017**, *678*, 79–84. [[CrossRef](#)]
118. Trummala, N.R.; Sutton, C.; Aziz, S.G.; Toney, M.F.; Risko, C.; Bredas, J.-L. Effect of solvent additives on the solution aggregation of phenyl-C₆₁-butyl acid methyl ester (PCBM). *Chem. Mater.* **2015**, *27*, 8261–8272. [[CrossRef](#)]
119. Paliy, M.; Consta, S.; Yang, J. Interactions between carbon nanoparticles in a droplet of organic solvent. *J. Phys. Chem. C* **2014**, *118*, 16074–16086. [[CrossRef](#)]
120. Banerjee, S. Molecular dynamics study of self-agglomeration of charged fullerenes in solvents. *J. Chem. Phys.* **2013**, *138*, 044318. [[CrossRef](#)] [[PubMed](#)]
121. Mortuza, S.M.; Kariyawasam, L.K.; Banerjee, S. Combined deterministic-stochastic framework for modeling the agglomeration of colloidal particles. *Phys. Rev. E* **2015**, *92*, 013304. [[CrossRef](#)]
122. Mortuza, S.M.; Banerjee, S. Molecular modeling study of agglomeration of [6,6]-phenyl-C₆₁-butyric acid methyl ester in solvents. *J. Chem. Phys.* **2012**, *137*, 244308. [[CrossRef](#)]
123. Mchedlov-Petrosyan, N.O.; Al-Shuuchi, Y.T.M.; Kamneva, N.N.; Marynin, A.I.; Klochkov, V.K. The interactions of the nanosized aggregates of fullerene C₆₀ with electrolytes in methanol: Coagulation and overcharging of particles. *Langmuir* **2016**, *32*, 10065–10072. [[CrossRef](#)]

124. Zulian, L.; Ruzicka, B.; Ruocco, G. About the formation of C₆₀ fine particles with reprecipitation method in ethanol/carbon disulfide mixture. *J. Photochem. Photobiol. A* **2007**, *187*, 402–405. [[CrossRef](#)]
125. Alfè, M.; Barbella, R.; Bruno, A.; Minutolo, P.; Ciajolo, A. Solution behaviour of C₆₀ fullerene in *N*-methylpyrrolidinone/toluene mixtures. *Carbon* **2005**, *43*, 665–667. [[CrossRef](#)]
126. Alfè, M.; Apicella, B.; Barbella, R.; Bruno, A.; Ciajolo, A. Aggregation and interactions of C₆₀ and C₇₀ fullerenes in neat *N*-methylpyrrolidinone and in *N*-methylpyrrolidinone/toluene mixtures. *Chem. Phys. Lett.* **2005**, *405*, 193–197. [[CrossRef](#)]
127. Stuart, E.J.E.; Tschulik, K.; Batchelor-McAuley, C.; Compton, R.G. Electrochemical observation of single collision events: Fullerene nanoparticles. *ACS Nano* **2014**, *8*, 7648–7654. [[CrossRef](#)] [[PubMed](#)]
128. Reichardt, C.; Welton, T. *Solvents and Solvent Effects in Organic Chemistry*; Wiley-VCH: Weinheim, Germany, 2011; 718p.
129. Kyzyma, O.A.; Mchedlov-Petrossyan, N.O.; Al-Shuuchi, Y.T.M.; Tropin, T.V.; Ivankov, O.I.; Kriklya, N.N.; Gromovoy, T.Y.; Kryshtal, A.P.; Zhigunov, A.N.; Korosteleva, E.A.; et al. Diluted and concentrated organosols of fullerene C₆₀ in the toluene–acetonitrile solvent system as studied by diverse experimental methods. *Fuller. Nanotub. Carbon Nanostruct.* **2021**, *29*, 315–330. [[CrossRef](#)]
130. Volmer, M. *Kinetik der Phasenbildung*; Russian Translation; Nauka: Moscow, Russia, 1986; Chapter 5.
131. Pille, U.; Herodes, K.; Leito, I.; Burk, P.; Pihl, V.; Koppel, I. Solvatochromism of fullerene C₆₀ in solvent mixtures: Application of the preferential solvation model. *Proc. Estonian Acad. Sci. Chem.* **2002**, *51*, 3–18.
132. Deguchi, S.; Mukai, S. Top-down preparation of dispersions of C₆₀ nanoparticles in organic solvents. *Chem. Lett.* **2006**, *35*, 396–397. [[CrossRef](#)]
133. Nonomura, Y.; Morita, Y.; Deguchi, S.; Mukai, S. Anomalously stable dispersions of graphite in water/acetone mixtures. *J. Colloid Int. Sci.* **2010**, *346*, 96–99. [[CrossRef](#)]
134. Yevlampieva, N.P.; Biryulin, Y.F.; Melenevskaja, E.Y.; Zgonnik, V.N.; Rjuntsev, E.I. Aggregation of fullerene C₆₀ in *N*-methylpyrrolidone. *Colloids Surf. A* **2002**, *209*, 167–171. [[CrossRef](#)]
135. Kyzyma, O.A.; Bulavin, L.A.; Aksenov, V.L.; Avdeev, M.V.; Tropin, T.V.; Korobov, M.V.; Snegir, S.V.; Rosta, L. Organization of fullerene clusters in the system C₆₀/*N*-methyl-2-pyrrolidone. *Mater. Struct.* **2008**, *15*, 17–20.
136. Kyzyma, O.A.; Korobov, M.V.; Avdeev, M.V.; Garamus, V.M.; Snegir, S.V.; Petrenko, V.I.; Aksenov, V.L.; Bulavin, L.A. Aggregate development in C₆₀ spectroscopy. *Chem. Phys. Lett.* **2010**, *493*, 103–106. [[CrossRef](#)]
137. Tropin, T.V.; Avdeev, M.V.; Kyzyma, O.A.; Yeregin, R.A.; Jargalan, N.; Korobov, M.V.; Aksenov, V.L. Towards description of kinetics of dissolution and cluster growth in C₆₀/*N*MMP solutions. *Phys. Status Solidi B* **2011**, *248*, 2728–2731. [[CrossRef](#)]
138. Kyrey, T.O.; Kyzyma, O.A.; Avdeev, M.V.; Tropin, T.V.; Korobov, M.V.; Aksenov, V.L.; Bulavin, L.A. Absorption characteristics of fullerene C₆₀ in *N*-methyl-2-pyrrolidone/toluene mixture. *Fuller. Nanotub. Carbon Nanostruct.* **2012**, *20*, 341–344. [[CrossRef](#)]
139. Karpenko, O.B.; Trachevskij, V.V.; Filonenko, O.V.; Lobanov, V.V.; Avdeev, M.V.; Tropin, T.V.; Kyzyma, O.A.; Snegir, S.V. NMR study of non-equilibrium state of fullerene C₆₀ in *N*-methyl-2-pyrrolidone. *Ukr. J. Phys.* **2012**, *57*, 860–863. [[CrossRef](#)]
140. Kyzyma, O.A.; Kyrey, T.O.; Avdeev, M.V.; Korobov, M.V.; Bulavin, L.A.; Aksenov, V.L. Non-reversible solvatochromism in *N*-methyl-2-pyrrolidone/toluene mixed solutions of fullerene C₆₀. *Chem. Phys. Lett.* **2013**, *556*, 178–181. [[CrossRef](#)]
141. Tropin, T.V.; Kyrey, T.O.; Kyzyma, O.A.; Feoktistov, A.V.; Avdeev, M.V.; Bulavin, L.A.; Rosta, L.; Aksenov, V.L. Experimental investigation of C₆₀/*N*MPP/toluene solutions by UV–Vis spectroscopy and small-angle neutron scattering. *J. Surf. Investig. X-ray Synchrotron Neutron Tech.* **2013**, *7*, 1–4. [[CrossRef](#)]
142. Tropin, T.V.; Jargalan, N.; Avdeev, M.V.; Kyzyma, O.A.; Sangaa, D.; Aksenov, V.L. Calculation of the distribution of clusters by size and SANS for C₆₀/*N*-methylpyrrolidone solutions. *Phys. Solid State Funct. Mater.* **2014**, *56*, 147–150. (In Russian)
143. Bulavin, L.A.; Nagorna, T.V.; Kyzyma, O.A.; Chudoba, D.; Ivankov, O.I.; Nagorny, V.I.; Avdeev, M.V. Fullerene clustering in C₇₀/*N*-methyl-2-pyrrolidone/toluene liquid system. *Ukr. J. Phys.* **2018**, *63*, 118–120. [[CrossRef](#)]
144. Snegir, S.V.; Tropin, T.V.; Kyzyma, O.A.; Kuzmenko, M.O.; Petrenko, V.I.; Garamus, V.M.; Korobov, M.V.; Avdeev, M.V.; Bulavin, L.A. On a specific state of C₆₀ fullerene in *N*-methyl-2-pyrrolidone solution: Mass spectrometric study. *Appl. Surf. Sci.* **2019**, *481*, 1566–1572. [[CrossRef](#)]
145. Nagorna, T.V.; Kyzyma, O.A.; Chuhoba, D.; Nagorny, A.V. Temporal solvatochromic effect in ternary C₇₀/toluene/*N*-methylpyrrolidone-2-one solution. *J. Mol. Liq.* **2017**, *235*, 111–114. [[CrossRef](#)]
146. Nagorna, T.V.; Kuzmenko, M.O.; Kyzyma, O.A.; Chudoba, D.; Nagorny, A.V.; Tropin, T.V.; Garamus, V.M.; Jazdzewska, M.; Bulavin, L.A. Structural reorganization of fullerene C₇₀ in *N*-methyl-2-pyrrolidone/toluene mixtures. *J. Mol. Liq.* **2018**, *272*, 948–952. [[CrossRef](#)]
147. Naumenko, A.; Biliy, M.; Gubanov, V.; Navozenko, A. Spectroscopic studies of fullerene clusters in *N*-methyl-2-pyrrolidone. *J. Mol. Liq.* **2017**, *235*, 115–118. [[CrossRef](#)]
148. Zhang, S.; Sakai, R.; Abe, T.; Iyoda, T.; Norimatsu, T.; Nagai, K. Photoelectrochemical and photocatalytic properties of biphasic organic p- and n-type semiconductor nanoparticles fabricated by a reprecipitation process. *ACS Appl. Mater. Interfaces* **2011**, *3*, 1902–1909. [[CrossRef](#)] [[PubMed](#)]
149. Sun, Y.-P.; Ma, B.; Lawson, G.E. Electron donor-acceptor interactions of fullerenes C₆₀ and C₇₀ with triethylamine. *Chem. Phys. Lett.* **1995**, *233*, 57–62. [[CrossRef](#)]
150. Datta, D.; Mukherjee, A.K. Aggregation of [70]fullerene in presence of acetonitrile: A chemical kinetic experiment. *J. Chem. Phys.* **2006**, *124*, 144509. [[CrossRef](#)] [[PubMed](#)]

151. Tropin, T.V.; Avdeev, M.V.; Jargalan, N.; Kuzmenko, M.O.; Aksenov, V.L. Kinetics of cluster growth in fullerene solutions of different polarity. In *Modern Problems of the Physics of Liquid Systems*; Bulavin, L.A., Xu, L., Eds.; Springer: Cham, Switzerland, 2019; pp. 249–272. [CrossRef]
152. Tropin, T.V.; Aksenov, V.L.; Schmelzer, J.W.P. Kinetic processes in fullerene solutions. Kinetics of cluster growth in fullerene solutions of different polarity. *Phys. Elem. Particl. Atomic Nucl.* **2021**, *52*, 615–644. (In Russian) [CrossRef]
153. Kolthoff, I.M. Acid-base equilibria in dipolar aprotic solvents. *Anal. Chem.* **1974**, *46*, 1992–2003. [CrossRef]
154. Mrzel, A.; Mertelj, A.; Omerzu, A.; Copic, M.; Mihailovic, D. Investigation of encapsulation and solvatochromism of fullerenes in binary solvent mixtures. *J. Phys. Chem. B* **1999**, *103*, 11256–11260. [CrossRef]
155. Hendrickson, O.D.; Pridvorova, S.M.; Safenkova, I.V.; Fedyunina, N.S.; Platonova, T.A.; Zherdev, A.V.; Dzantiev, B.B. Characterization of fullerene C₆₀ dispersions by transparent electron microscopy. *Mod. Public Sci. Educ.* **2013**, 1–7. Available online: https://www.researchgate.net/publication/309900808_Characterization_of_fullerene_C60_dispersions_by_transparent_electron_microscopy_in_Russian (accessed on 10 October 2023). (In Russian).
156. Yang, S.; Mulet, X.; Gengenbach, T.; Waddington, L.; Seeber, A.; Zhen, M.; Wang, C.; Muia, B.W.; Such, G.K.; Hao, X. Limitations with solvent exchange methods for synthesis of colloidal fullerenes. *Colloids Surf. A* **2017**, *514*, 21–31. [CrossRef]
157. Kolthoff, I.M.; Chantooni, M.K.; Smagowski, H. Acid-base strength in *N,N*-dimethylformamide. *Anal. Chem.* **1970**, *42*, 1622–1628. [CrossRef]
158. Delgado, A.V.; González-Caballero, F.; Hunter, R.J.; Koopal, L.K.; Lyklema, J. Measurement and interpretation of electrokinetic phenomena. *J. Colloid Int. Sci.* **2007**, *309*, 194–224. [CrossRef]
159. Ohshima, H. A simple expression for Henry's function for the retardation effect in electrophoresis of spherical colloidal particles. *J. Colloid Int. Sci.* **1994**, *168*, 269–271. [CrossRef]
160. Mchedlov-Petrosyan, N.O.; Kamneva, N.N.; Al-Shuuchi, Y.T.M.; Marynin, A.I. Interaction of C₆₀ aggregates with electrolytes in acetonitrile. *Colloids Surf. A* **2017**, *516*, 345–353. [CrossRef]
161. Chaban, V.V.; Maciel, C.; Fileti, E.E. Solvent polarity considerations are unable to describe fullerene solvation behavior. *J. Phys. Chem. B* **2014**, *118*, 3378–3384. [CrossRef] [PubMed]
162. Maciel, C.; Fileti, E.E. Molecular interactions between fullerene C₆₀ and ionic liquids. *Chem. Phys. Lett.* **2013**, *568*, 75–79. [CrossRef]
163. Chaban, V.V.; Maciel, C.; Fileti, E.E. Does like dissolves like rule hold for fullerene and ionic liquids? *J. Solut. Chem.* **2014**, *43*, 1019–1031. [CrossRef]
164. Fileti, E.E.; Chaban, V.V. Structure and supersaturation of highly concentrated solutions of buckyball in 1-butyl-3-methylimidazolium tetrafluoroborate. *J. Phys. Chem. B* **2014**, *118*, 7376–7382. [CrossRef]
165. Fileti, E.E.; Chaban, V.V. Imidazolium ionic liquid helps to disperse fullerenes in water. *J. Phys. Chem. Lett.* **2014**, *5*, 1795–1800. [CrossRef]
166. García, G.; Atilhan, M.; Aparicio, S. Theoretical study on the solvation of C₆₀ fullerene by ionic liquids. *J. Phys. Chem. B* **2014**, *118*, 11330–11340. [CrossRef]
167. García, G.; Atilhan, M.; Aparicio, S. Theoretical study on the solvation of C₆₀ fullerene by ionic liquids II: DFT analysis of the interaction mechanism. *J. Phys. Chem. B* **2015**, *119*, 10616–10629. [CrossRef]
168. Szala-Bilnik, J.; Costa Gomes, M.F.; Pádua, A.A.H. Solvation of C₆₀ fullerene and C₆₀F₄₈ fluorinated fullerene in molecular and ionic liquids. *J. Phys. Chem. C* **2016**, *120*, 19396–19408. [CrossRef]
169. Costa Gomes, M.F.; Pison, L.; Padua, A.A.H. Experimental study of the interactions of fullerene with ionic liquids. In *Ionic Liquids: Current State and Future Directions*; ACS Symposium Series; American Chemical Society: Washington, DC, USA, 2017; Volume 1250, pp. 273–281. [CrossRef]
170. Ahmad, Y.; Andanson, J.-M.; Bonnet, P.; Batisse, N.; Claves, D.; Dubois, M.; Padua, A. Fluorination effect on the solubility of C₆₀ in a bis(trifluoromethylsulfonyl)imide based ionic liquid. *Colloids Surf. A* **2022**, *649*, 129140. [CrossRef]
171. Martins, S.; Fedorov, A.; Afonso, C.A.M.; Baleizão, C.; Berberan-Santos, M.N. Fluorescence of fullerene C₇₀ in ionic liquids. *Chem. Phys. Lett.* **2010**, *497*, 43–47. [CrossRef]
172. Cardoso, W.B.; Colherinhas, G. Fullerene C₆₀ spectroscopy in [BMIM][PF₆] ionic liquid: Molecular dynamics study using polarization effects. *J. Mol. Struct.* **2022**, *1250*, 131887. [CrossRef]
173. Bright, F.V.; Baker, G.A. Comment on “How polar are ionic liquids? Determination of the static dielectric constant of an imidazolium-based ionic liquid by microwave dielectric spectroscopy”. *J. Phys. Chem. B* **2006**, *110*, 5822–5823. [CrossRef] [PubMed]
174. Wakai, C.; Oleinikova, A.; Weingärtner, H. Reply to “Comment on ‘How polar are ionic liquids? Determination of the static dielectric constant of an imidazolium-based ionic liquid by microwave spectroscopy’”. *J. Phys. Chem. B* **2006**, *110*, 5824. [CrossRef]
175. Campisciano, V.; La Parola, V.; Liotta, L.F.; Giacalone, F.; Gruttadauria, M. Fullerene–ionic-liquid conjugates: A new class of hybrid materials with unprecedented properties. *Chem. Eur. J.* **2015**, *21*, 1–9. [CrossRef] [PubMed]
176. Mikheev, I.V.; Sozarukova, M.M.; Izmailov, D.Y.; Kareev, I.E.; Proskurnina, E.V.; Proskurnin, M.A. In vitro antioxidant potential evaluation of non-functionalized fullerenes and endofullerene. *Preprint.org* **2021**. [CrossRef]
177. Ritter, U.; Nikolenko, A.; Aliksandrov, M.; Strelchuk, V.; Chumachenko, V.; Kutsevol, N.V.; Scharff, P.; Prylutskyy, Y.I. Structural and optical properties of C₇₀ fullerenes in aqueous solution. *Fuller. Nanotub. Carbon Nanostruct.* **2023**, *31*, 983–988. [CrossRef]
178. Gigault, J.; Balaresque, M.; Tabuteau, H. Estuary-on-a-chip: Unexpected results for nanoparticles fate and transport. *Environ. Sci. Nano* **2018**, *5*, 1231–1236. [CrossRef]

179. Mashayekhi, H. Aggregation and Coagulation of C₆₀ Fullerene as Affected by Natural Organic Matter and Ionic Strength. Ph.D. Thesis, Graduate School of the University of Massachusetts, Amherst, MA, USA, 2016. [CrossRef]
180. Chen, C. Aggregation and Adsorption Processes of Carbonaceous Nanoparticles in Aqueous Environments. Ph.D. Thesis, The State University of New Jersey, New Brunswick, NJ, USA, October 2017; 251p. Available online: <https://rucore.libraries.rutgers.edu/rutgers-lib/55387/> (accessed on 10 October 2023).
181. Scrivens, W.A.; Tour, J.M.; Creek, K.E.; Pirisi, L. Synthesis of ¹⁴C-labeled C₆₀, its suspension in water, and its uptake by human keratinocytes. *J. Am. Chem. Soc.* **1994**, *116*, 4517–4518. [CrossRef]
182. Brant, J.; Lecoanet, H.; Hotze, M.; Wiesner, M. Comparison of electrokinetic properties of colloidal fullerenes (n-C₆₀) formed using two procedures. *Environ. Sci. Technol.* **2005**, *39*, 6343–6351. [CrossRef] [PubMed]
183. Marples, R.D.; Hilburn, M.E.; Murdianti, B.S.; Hikkaduwa Koralege, R.S.; Williams, J.S.; Kuriyavar, S.I.; Ausman, K.D. Optimized solvent-exchange synthesis method for C₆₀ colloidal dispersions. *J. Colloid Int. Sci.* **2012**, *370*, 27–31. [CrossRef] [PubMed]
184. Deguchi, S.; Algarova, R.Z.; Tsujii, K. Stable dispersions of fullerenes, C₆₀ and C₇₀, in water. Preparation and characterization. *Langmuir* **2001**, *17*, 6013–6017. [CrossRef]
185. Wu, J.; Benoit, D.; Lee, S.S.; Li, W.; Fortner, J.D. Ground state reactions of nC₆₀ with free chlorine in water. *Environ. Sci. Technol.* **2016**, *50*, 721–731. [CrossRef] [PubMed]
186. Kyzyma, O.A.; Avdeev, M.V.; Bolshakova, O.I.; Melentev, P.; Sarantseva, S.V.; Ivankov, O.I.; Korobov, M.V.; Mikheev, I.V.; Tropin, T.V.; Kubovcikova, M.; et al. State of aggregation and toxicity of aqueous fullerene solutions. *Appl. Surf. Sci.* **2019**, *483*, 69–75. [CrossRef]
187. Hilburn, M.E.; Murdianti, B.S.; Marples, R.D.; Williams, J.S.; Damron, J.T.; Kuriyavar, S.I.; Ausman, K.D. Synthesizing aqueous fullerene colloidal suspensions by new solvent-exchange methods. *Colloids Surf. A* **2012**, *401*, 48–51. [CrossRef]
188. Tseluikin, V.N.; Tolstova, I.V.; Gun'kin, I.F.; Pankst'yanov, A.Y. Preparation of aqueous colloidal dispersion of C₆₀ fullerene. *Colloid J.* **2005**, *67*, 522–523. [CrossRef]
189. Tseluikin, V.N.; Chubenko, I.S.; Gun'kin, I.F.; Pankst'yanov, A.Y. Colloidal dispersion of fullerene C₆₀ free of organic solvents. *Russ. J. Appl. Chem.* **2006**, *79*, 325–326. [CrossRef]
190. Tseluikin, V.N.; Kanaf'eva, O.A.; Nevernaya, O.G. About water dispersions of C₆₀ fullerene. *Condens. Matter Interphases* **2012**, *14*, 390–392.
191. Wei, X.; Wu, M.; Qi, L.; Xu, Z. Selective solution-phase generation and oxidation reaction of C₆₀ⁿ⁻ (n = 1,2) and formation of an aqueous colloidal solution of C₆₀. *J. Chem. Soc. Perkin Trans.* **1997**, *2*, 1389–1394. [CrossRef]
192. Damasceno, J.P.V.; Hof, F.; Chauvet, O.; Zarbin, A.J.G.; Pénicaud, A. The role of functionalization on the colloidal stability of aqueous fullerene C₆₀ dispersions prepared with fullerides. *Carbon* **2021**, *173*, 1041–1047. [CrossRef]
193. Damasceno, J.P.V.; Kubota, L.T. From radicals destabilization to stable fullerene nanoaggregates. *Carbon Trends* **2022**, *9*, 100226. [CrossRef]
194. Andrievsky, G.V.; Kosevich, M.V.; Vovk, O.M.; Shelkovsky, V.S.; Vashchenko, L.A. On the production of an aqueous colloidal solution of fullerenes. *J. Chem. Soc. Chem. Commun.* **1995**, *12*, 1281–1282. [CrossRef]
195. Belousov, V.P.; Belousova, I.M.; Kris'ko, A.V.; Kris'ko, T.K.; Murav'eva, T.D.; Sirotkin, A.K. Aqueous micellar solution of C₆₀: Preparation, properties, and capability for generation of singlet oxygen. *Russ. J. Gen. Chem.* **2006**, *76*, 251–257. [CrossRef]
196. Aich, N.; Flora, J.R.V.; Saleh, N.B. Preparation and characterization of stable aqueous higher-order fullerenes. *Nanotechnology* **2012**, *23*, 055705. [CrossRef] [PubMed]
197. Mikheev, I.V.; Bolotnik, T.A.; Volkov, D.S.; Korobov, M.V.; Proskurnin, M.A. Approaches to the determination of C₆₀ and C₇₀ fullerene and their mixtures in aqueous and organic solutions. *Nanosyst. Phys. Chem. Math.* **2016**, *7*, 104–110. [CrossRef]
198. Marfunin, M.O.; Klochkov, V.K.; Radionov, P.M.; Mchedlov-Petrossyan, N.O. Hydrosol of C₇₀ fullerene: Synthesis and stability in electrolytic solutions. *Ukr. Chem. J.* **2021**, *87*, 63–73. [CrossRef]
199. Zhang, L.; Zhao, Q.; Wang, S.; Mashayekhi, H.; Li, X.; Xing, B. Influence of ions on the coagulation and removal of fullerene in aqueous phase. *Sci. Total Environ.* **2014**, *466/467*, 604–608. [CrossRef]
200. Yang, Y.; Nakada, N.; Nakajima, R.; Wang, C.; Tanaka, H. Toxicity of aqueous fullerene nC₆₀ to activated sludge: Nitrification inhibition and microtox test. *J. Nanomater.* **2012**, *2012*, 512956. [CrossRef]
201. Kyzyma, E.A.; Kuz'menko, M.O.; Bulavin, L.A.; Petrenko, V.I.; Mikheev, I.V.; Zabolotny, M.A.; Kubovchikova, M.; Kopcansky, P.; Korobov, M.V.; Avdeev, M.V.; et al. Impact of a physiological medium on the aggregation state of C₆₀ and C₇₀ fullerenes. *J. Surf. Investig. X-ray Synchrotron Neutron Tech.* **2016**, *10*, 1125–1128. [CrossRef]
202. Li, B.; Yao, M.; Li, C.; Du, M.; Liu, B. Synthesis of water-soluble C₆₀ nanoparticles under ultrasonication and investigation of their photoluminescence property. *Chem. J. Chin. Univ.* **2014**, *35*, 949–953. [CrossRef]
203. Xia, X.R.; Monteiro-Riviere, N.A.; Riviere, J.E. Intrinsic biological property of colloidal fullerene nanoparticles (nC₆₀): Lack of lethality after high dose exposure to human epidermal and bacterial cells. *Toxicol. Lett.* **2010**, *197*, 128–134. [CrossRef] [PubMed]
204. Haftka, J.J.H.; Bauerlein, P.S.; Emke, E.; Lammertse, N.; Belokhovstova, D.; Hilvering, B.; de Voogt, P.; ter Laak, T.L. Colloidal stability of (functionalised) fullerenes in the presence of dissolved organic carbon and electrolytes. *Environ. Sci. Nano* **2015**, *2*, 280–287. [CrossRef]
205. Pospisil, L.; Gal, M.; Hromadova, M.; Bulíčková, J.; Kolivoška, V.; Cvačka, J.; Nováková, K.; Kavan, L.; Zukalová, M.; Dunsch, L. Search for the form of fullerene C₆₀ in aqueous medium. *Phys. Chem. Chem. Phys.* **2010**, *12*, 14095–14101. [CrossRef] [PubMed]

206. Mikheev, I.V. Development of Approaches to the Chemical Analysis of Aqueous Dispersions of Unmodified Fullerenes. PhD Thesis, Moscow State University, Moscow, Russia, 2018. (In Russian).
207. Mikheev, I.V.; Kareev, I.E.; Bubnov, V.P.; Volkov, D.S.; Korobov, M.V.; Proskurnin, M.A. Development of standard reference samples of aqueous fullerene dispersions. *J. Anal. Chem.* **2018**, *73*, 837–846. [CrossRef]
208. Isaacson, C.; Zhang, W.; Powell, T.; Ma, X.; Bouchard, D. Temporal changes in aqu/C₆₀ physical–chemical, deposition, and transport characteristics in aqueous systems. *Environ. Sci. Technol.* **2011**, *45*, 5170–5177. [CrossRef] [PubMed]
209. Murdianti, B.S.; Damron, J.T.; Hilburn, M.E.; Maples, R.D.; Hikkaduwa Koralege, R.S.; Kuriyavar, S.I.; Ausman, K.D. C₆₀ oxide as a key component of aqueous C₆₀ colloidal suspensions. *Environ. Sci. Technol.* **2012**, *46*, 7446–7453. [CrossRef] [PubMed]
210. Chang, X.; Vikesland, P.J. Uncontrolled variability in the extinction spectra of C₆₀ nanoparticle suspensions. *Langmuir* **2013**, *29*, 9685–9693. [CrossRef]
211. Chang, X.; Duncan, L.K.; Jinschek, J.; Vikesland, P.J. Alteration of nC₆₀ in the presence of environmentally relevant carboxylates. *Langmuir* **2012**, *28*, 7620–7633. [CrossRef]
212. Sugiyama, T.; Ryo, S.-I.; Oh, I.; Asaahi, T.; Masuhara, H. Nanosecond laser preparation of C₆₀ aqueous nanocolloids. *J. Photochem. Photobiol. A* **2009**, *207*, 7–12. [CrossRef]
213. Deguchi, S.; Mukai, S.-A.; Yamazaki, T.; Tsudome, M. Nanoparticles of fullerene C₆₀ from engineering of antiquity. *J. Phys. Chem. C* **2010**, *114*, 849–856. [CrossRef]
214. Deguchi, S.; Mukai, S.-A.; Sakaguchi, H.; Nonomura, Y. Non-engineered nanoparticles of C₆₀. *Sci. Rep.* **2013**, *3*, 2094. [CrossRef] [PubMed]
215. Chang, X.; Vikesland, P. UV–vis spectroscopic properties of nC₆₀ produced via extended mixing. *Environ. Sci. Technol.* **2011**, *45*, 9967–9974. [CrossRef] [PubMed]
216. Kato, H.; Nakamura, A.; Takahashi, K.; Kinugasa, S. Size effect on UV-Vis absorption properties of colloidal C₆₀ particles in water. *Phys. Chem. Chem. Phys.* **2009**, *11*, 4946–4948. [CrossRef] [PubMed]
217. Marinova, K.G.; Alargova, R.G.; Denkov, N.D.; Velev, O.D.; Petsev, D.N.; Ivanov, I.B.; Borwankar, B.P. Charging of oil–water interfaces due to spontaneous adsorption of hydroxyl ions. *Langmuir* **1996**, *12*, 2045–2051. [CrossRef]
218. Beattie, J.K.; Djerdjev, A.M. The pristine oil/water interface: Surfactant-free hydroxide-charged emulsions. *Angew. Chem. Int. Ed.* **2004**, *43*, 3568–3571. [CrossRef] [PubMed]
219. Mchedlov-Petrosyan, N.O.; Klochkov, V.K.; Andrievsky, G.V.; Shumakher, A.S.; Kleshchevnikova, V.N.; Koval, V.L.; Shapovalov, S.A.; Derevyanko, N.A.; Ishchenko, A.A. Interaction of polymethine dyes with fullerene C₆₀ hydrosol. *Sci. Appl. Photo.* **2001**, *43*, 1–13.
220. Choi, J.I.; Snow, S.D.; Kim, J.-H.; Jang, S.S. Interaction of C₆₀ with water: First-principles modeling and environmental implications. *Environ. Sci. Technol.* **2015**, *49*, 1529–1536. [CrossRef]
221. Noneman, K.; Muhich, C.; Ausman, K.; Henry, M.; Jankowski, E. Molecular simulations for understanding the stabilization of fullerenes in water. *J. Comput. Sci. Educ.* **2021**, *12*, 39–48. [CrossRef]
222. Hinkle, K.R.; Phelan, F.R., Jr. Solvation of carbon nanoparticles in water/alcohol mixtures: Using molecular simulation to probe energetics, structure, and dynamics. *J. Phys. Chem. C* **2017**, *121*, 22926–22938. [CrossRef]
223. Voronin, D.P.; Buchelnikov, A.S.; Kostjukov, V.V.; Khrapaty, S.V.; Wyrzykowski, D.; Piosik, J.; Prylutsky, Y.I.; Ritter, U.; Evstigneev, M.P. Evidence of entropically driven C₆₀ fullerene aggregation in aqueous solution. *J. Chem. Phys.* **2014**, *140*, 104909. [CrossRef] [PubMed]
224. Godínez-Pastor, J.L.; González-Melchor, M. Behavior of the fullerene/water system under liquid and liquid–vapor conditions: A molecular dynamics approach. *Chem. Phys.* **2023**, *574*, 112025. [CrossRef]
225. Kolker, A.M.; Borovkov, N.Y. Three-dimensional aggregation of fullerene C₆₀ at the air–water interface. *Colloids Surf. A* **2012**, *414*, 433–439. [CrossRef]
226. Mikheev, I.V.; Khimich, E.S.; Rebrikova, A.T.; Volkov, D.S.; Proskurnin, M.A.; Korobov, M.V. Quasi-equilibrium distribution of pristine fullerenes C₆₀ and C₇₀ in a water–toluene system. *Carbon* **2017**, *111*, 191–197. [CrossRef]
227. Jafvert, C.T.; Kulkarni, P.P. Buckminsterfullerene’s (C₆₀) octanol-water partition coefficient (Kow) and aqueous solubility. *Environ. Sci. Technol.* **2008**, *42*, 5945–5950. [CrossRef] [PubMed]
228. Final Project Report Partitioning of Nanoparticles into Organic Phases and Model Cells. Program Manager: Daniel W. Drell. Available online: <https://www.osti.gov/servlets/purl/1023025> (accessed on 10 October 2023).
229. Praetorius, A.; Tufenkji, N.; Goss, K.-U.; Scheringer, M.; von der Kammer, F.; Elimelech, M. The road to nowhere: Equilibrium partition coefficients for nanoparticles. *Environ. Sci. Nano* **2014**, *1*, 317–323. [CrossRef]
230. Hill, T.L. *Thermodynamics of Small Systems*; Bengamin, Ed.; Courier Corporation: New York, NY, USA, 1963; 210p.
231. Shchukin, E.D.; Pertsov, A.V.; Amelina, E.A.; Zelenev, A.S. *Colloid and Surface Chemistry*; Elsevier: Amsterdam, The Netherlands, 2001; 748p.
232. Scharff, P.; Risch, K.; Carta-Abelmann, L.; Dmytruk, I.M.; Bilyi, M.M.; Golub, O.A.; Khavryuchenko, A.V.; Buzaneva, E.V.; Aksenov, V.L.; Avdeev, M.V.; et al. Structure of C₆₀ fullerene in water: Spectroscopic data. *Carbon* **2004**, *42*, 1203–1206. [CrossRef]
233. Mchedlov-Petrosyan, N.O.; Klochkov, V.K.; Andrievsky, G.V. Colloidal dispersions of fullerene in water: Some properties and regularities of coagulation by electrolytes. *J. Chem. Soc. Faraday Trans.* **1997**, *93*, 4343–4346. [CrossRef]
234. Walther, J.H.; Jaffe, R.L.; Kotsalis, E.M.; Werder, T.; Halicioglu, T.; Koumoutsakos, P. Hydrophobic hydration of C₆₀ and carbon nanotubes in water. *Carbon* **2004**, *42*, 1185–1194. [CrossRef]

235. Fang, H.; Shen, B.-B.; Jing, J.; Lu, J.-L.; Wang, Y. Stability of C₆₀ nanoparticles in aquatic systems. *Environ. Sci.* **2014**, *35*, 1337–1342.
236. Chen, K.L.; Elimelech, M. Influence of humic acid on the aggregation kinetics of fullerene (C₆₀) nanoparticles in monovalent and divalent electrolyte solutions. *J. Colloid Int. Sci.* **2007**, *309*, 126–134. [[CrossRef](#)] [[PubMed](#)]
237. Aich, N.; Boateng, L.K.; Sabaraya, I.V.; Das, D.; Flora, J.R.V.; Saleh, N.B. Aggregation kinetics of higher-order fullerene clusters in aquatic systems. *Environ. Sci. Technol.* **2016**, *50*, 3562–3571. [[CrossRef](#)] [[PubMed](#)]
238. Zhang, L.; Zhang, Y.-k.; Lin, X.-c.; Yang, K.; Lin, D.-h. The role of humic acid in stabilizing fullerene (C₆₀) suspensions. *J. Zhejiang Univ. Sci. A* **2014**, *15*, 634–642. [[CrossRef](#)]
239. Qu, X.; Hwang, Y.S.; Alvarez, P.J.J.; Bouchard, D.; Li, Q. UV irradiation and humic acid mediate aggregation of aqueous fullerene (nC₆₀) nanoparticles. *Environ. Sci. Technol.* **2010**, *44*, 7821–7826. [[CrossRef](#)] [[PubMed](#)]
240. Chen, K.L.; Elimelech, M. Aggregation and deposition kinetics of fullerene (C₆₀) nanoparticles. *Langmuir* **2006**, *22*, 10994–11001. [[CrossRef](#)] [[PubMed](#)]
241. Chen, K.L.; Elimelech, M. Relating colloidal stability of fullerene (C₆₀) nanoparticles to nanoparticle charge and electrokinetic properties. *Environ. Sci. Technol.* **2009**, *43*, 7270–7276. [[CrossRef](#)] [[PubMed](#)]
242. Meng, Z.; Hashmi, S.M.; Elimelech, M. Aggregation rate and fractal dimension of fullerene nanoparticles via simultaneous multiangle static and dynamic light scattering measurement. *J. Colloid Int. Sci.* **2013**, *392*, 27–33. [[CrossRef](#)] [[PubMed](#)]
243. Khokhrakov, A.A.; Kyzyma, O.A.; Bulavin, L.A.; Len, A.; Avdeev, M.V.; Aksenov, V.L. Colloidal structure and stabilization mechanism of aqueous solutions of unmodified fullerene C₆₀. *Crystallogr. Rep.* **2007**, *52*, 487–491. [[CrossRef](#)]
244. Derjaguin, B.V.; Landau, L. Theory of the stability of strongly charged lyophobic sols and of the adhesion of strongly charged particles in solutions of electrolytes. *Acta Phys. Chim. URSS* **1941**, *14*, 633–662. [[CrossRef](#)]
245. Dukhin, S.S.; Derjaguin, B.V.; Semnikhin, N.M. The interaction of two identical spherical colloidal particles in large distances. *Doklady AN USSR* **1970**, *192*, 357–360. (In Russian)
246. Derjaguin, B.V.; Churaev, N.V.; Muller, V.M. *Surface Forces*; Nauka: Moscow, Russia, 1985; 398p. (In Russian)
247. Tadros, T. General principles of colloid stability and the role of surface forces. In *Colloid Stability: The Role of Surface Forces, Part I*; Tadros, T.F., Ed.; Wiley-VCH Verlag GmbH & Co. KGaA: Weinheim, Germany, 2014; Volume 1, pp. 1–22. [[CrossRef](#)]
248. Israelachvili, J.N. *Intermolecular and Surface Forces*, 3rd ed.; Academic Press: New York, NY, USA, 2011; 674p.
249. Trefalt, G.; Szilagyi, I.; Borkovec, M. Poisson–Boltzmann description of interaction forces and aggregation rates involving charged colloidal particles in asymmetric electrolytes. *J. Colloid Int. Sci.* **2013**, *406*, 111–120. [[CrossRef](#)]
250. Oncsik, T.; Trefalt, G.; Csendes, Z.; Szilagyi, I.; Borkovec, M. Aggregation of negatively charged colloidal particles in the presence of multivalent cations. *Langmuir* **2014**, *30*, 733–741. [[CrossRef](#)] [[PubMed](#)]
251. Zhang, Z.; Zhao, L.; Li, Y.; Chu, M. A modified method to calculate critical coagulation concentration based on DLVO theory. *Math. Probl. Eng.* **2015**, *2015*, 317483. [[CrossRef](#)]
252. Wiese, G.R.; Healy, T.W. Effect of particle size on colloid stability. *Trans. Faraday Soc.* **1970**, *66*, 490–499. [[CrossRef](#)]
253. Hogg, R.; Healy, T.W.; Fuerstenau, D.W. Mutual coagulation of colloidal dispersions. *Trans. Faraday Soc.* **1966**, *62*, 1638–1651. [[CrossRef](#)]
254. Katacharu, K. *Interfacial Chemistry*; Russian Translation; Tamaru, K., Ed.; Mir: Moscow, Russian, 1983; 272p.
255. Ravindran, S.; Wu, J. Overcharging of nanoparticles in electrolyte solutions. *Langmuir* **2004**, *20*, 7333–7338. [[CrossRef](#)] [[PubMed](#)]
256. Lyklema, J. Overcharging, charge reversal: Chemistry or physics? *Colloids Surf. A* **2006**, *291*, 3–12. [[CrossRef](#)]
257. Churaev, N.V.; Derjaguin, B.V. Inclusion of structural forces in the theory of stability of colloids and films. *J. Colloid Int. Sci.* **1985**, *103*, 542–553. [[CrossRef](#)]
258. Cao, T.; Szilagyi, I.; Oncsik, T.; Borkovec, M.; Trefalt, G. Aggregation of colloidal particles in the presence of multivalent co-ions: The inverse Schulze–Hardy rule. *Langmuir* **2015**, *31*, 6610–6614. [[CrossRef](#)]
259. Kruyt, H.R. (Ed.) *Colloid Science*; Elsevier: Amsterdam, The Netherlands, 1952; 245p.
260. Laguta, A.N.; Mchedlov-Petrosyan, N.O.; Bogatyrenko, S.I.; Kovalenko, S.M.; Bunyatyan, N.D.; Trostianko, P.V.; Karbivskii, V.L.; Filatov, D.Y. Interaction of aqueous suspensions of single-walled oxidized carbon nanotubes with inorganic and organic electrolytes. *J. Mol. Liq.* **2022**, *347*, 117948. [[CrossRef](#)]
261. Sano, M.; Kamino, A.; Shinkai, S. Critical coagulation of Langmuir monolayers: 2D Schulze–Hardy rule. *J. Phys. Chem. B* **2000**, *104*, 10339–10347. [[CrossRef](#)]
262. Burton, E.F.; Bishop, E. Coagulation of colloidal solutions by electrolytes: Influence of concentration of sol. *J. Phys. Chem.* **1920**, *24*, 701–715. [[CrossRef](#)]
263. Fisher, E.; Sorum, C.H. Chromium hydroxide hydrosols and the Burton–Bishop rule. *J. Phys. Chem.* **1934**, *39*, 283–287. [[CrossRef](#)]
264. Tamamushi, B.; Tamaki, K. The action of long-chain cations on negative silver iodine sol. *Kolloid-Z.* **1959**, *163*, 122–126. [[CrossRef](#)]
265. Mukherjee, J.N.; Sen, N.N. Coagulation of metal sulphide hydrosols. Part I. Influence of distance between the particles of a sol on its stability. Anomalous protective action of dissolved hydrogen sulphide. *J. Chem. Soc. Faraday Trans.* **1919**, *115*, 461–472. [[CrossRef](#)]
266. Tamamushi, B. The action of surface active large ions on the stability of hydrophobic colloids. *Kolloid-Z.* **1957**, *150*, 44–49. [[CrossRef](#)]
267. Wang, W.; Gu, B.; Liang, L.; Hamilton, W.B. Adsorption and Structural Arrangement of Cetyltrimethylammonium Cations at the Silica Nanoparticle–Water Interface. *J. Phys. Chem. B* **2004**, *108*, 17477–17483. [[CrossRef](#)]

-
268. Laguta, A.N.; Mchedlov-Petrosyan, N.O.; Kovalenko, S.M.; Voloshina, T.O.; Haidar, V.I.; Filatov, D.Y.; Trostyanko, P.V.; Karbivski, V.L.; Bogatyrenko, S.I.; Xu, L.; et al. Stability of aqueous suspensions of COOH-decorated carbon nanotubes to organic solvents, esterification, and decarboxylation. *J. Phys. Chem. Lett.* **2022**, *13*, 10126–10131. [[CrossRef](#)]
269. Mchedlov-Petrosyan, N.O.; Kriklya, N.N.; Laguta, A.N.; Ōsawa, E. Stability of detonation nanodiamond colloid with respect to inorganic electrolytes and anionic surfactants and solvation of the particles surface in DMSO–H₂O organo-hydrosols. *Liquids* **2022**, *2*, 196–209. [[CrossRef](#)]

Disclaimer/Publisher’s Note: The statements, opinions and data contained in all publications are solely those of the individual author(s) and contributor(s) and not of MDPI and/or the editor(s). MDPI and/or the editor(s) disclaim responsibility for any injury to people or property resulting from any ideas, methods, instructions or products referred to in the content.